Chapter 3

Alternating Direction Implicit Approach for the Two-Dimensional Time-Fractional Nonlinear Klein-Gordon and Sine-Gordon Problems

In this chapter, an numerical scheme is established to achieve the theoretical accuracy near the weak singularity at $t = 0$ in solving the two-dimensional nonlinear time-fractional mixed diffusion and diffusion-wave (TFMDW) equation. The governing problem involves diffusion term with TFCD of order β $(0 < \beta < 1)$, and wave term with TFCD of order α $(1 < \alpha < 2)$. The linearized $L1$ method is used to discretize both the TFCDs on nonuniform time meshes and central difference operator for the space derivative approximation, the considered problem is converted to an

equivalent system of equations. Further, the unconditional stability analysis is discussed. Numerical examples are given for 1D and 2D nonlinear TFMDW equations with smooth and non-smooth exact solutions to describe the accuracy of numerical scheme.

3.1 Introduction

In this chapter, we analyzed and discussed the numerical scheme for solving the following $2D$ time fractional nonlinear mixed diffusion and diffusion-wave equation:

$$ {}^{C}\mathcal{D}^{\beta}_{0,t}u + {}^{C}\mathcal{D}^{\alpha}_{0,t}u + F(u) = \frac{\partial^2 u}{\partial x^2} + \frac{\partial^2 u}{\partial y^2} + f(x,y,t), \quad (x,y,t) \in \Omega \times (0,T], \tag{3.1} $$

$$ u(x,y,0) = \phi(x,y), \qquad \frac{\partial u(x,y,0)}{\partial t} = \varphi(x,y), \quad (x,y) \in \Omega, \tag{3.2} $$

$$ u(x,y,t) = \Phi(x,y,t), \qquad (x,y,t) \in \partial\Omega \times (0,T], \tag{3.3} $$

where, $\Omega = (0, L_1) \times (0, L_2)$, $\overline{\Omega} = \Omega \cup \partial\Omega$, $\phi \in C(\overline{\Omega})$, $\varphi \in C(\overline{\Omega})$, $\Phi \in C(\overline{\Omega} \times [0,T])$, and $f \in C(\overline{\Omega} \times [0,T])$, where $\overline{\Omega} \times [0,T] := [0, L_1] \times [0, L_2] \times [0,T]$. Furthermore, the operators ${}^{C}\mathcal{D}^{\beta}_{0,t}$, ${}^{C}\mathcal{D}^{\alpha}_{0,t}$ denotes the TFCDs of order β $(0 < \beta < 1)$ and α $(1 < \alpha < 2)$, respectively. The TFCDs of a function u [14] are defined as:

$$ {}^{C}\mathcal{D}^{\beta}_{0,t}u(x,y,t) = \frac{1}{\Gamma(1-\beta)} \int_0^t (t-s)^{-\beta} \frac{\partial u(x,y,s)}{\partial s}\, ds, \quad \beta \in (0,1), \tag{3.4} $$

$$ {}^{C}\mathcal{D}^{\alpha}_{0,t}u(x,y,t) = \frac{1}{\Gamma(2-\alpha)} \int_0^t (t-s)^{1-\alpha} \frac{\partial^2 u(x,y,s)}{\partial s^2}\, ds, \quad \alpha \in (1,2). \tag{3.5} $$

When $\beta = 1$ and $\alpha = 2$, then (3.1) converts into the classical telegraph equation. Here, the second-order derivative (i.e. $\partial_{tt}u$) characterizes the wave-type behavior, while the first-order derivative (i.e. $\partial_t u$) shows as diffusion like behavior. The

mixed diffusion and diffusion-wave equation can be employed to investigate the intermediate processes between diffusion and diffusion-wave equations. The considered problem (3.1) is generalization of the time-fractional telegraph equation. Suppose the function $F(u(x,y,t))$ satisfies the Lipschitz condition with respect to u with Lipschitz constant $\mathcal{L}$, then

$$|F(u) - F(\bar{u})| \leq \mathcal{L}|u - \bar{u}|, \quad \forall u,\ \bar{u}. \tag{3.6}$$

The problem (3.1) contains both time-fractional diffusion (or sub-diffusion) and the time-fractional wave equation (or super-diffusion) terms together, due to which it becomes more challenging to develop computational algorithm for solving higher dimension problems. Also it is difficult task to find the analytical solutions of such type problems.

In the literature, few research articles are available on the uniform meshes to solve the linear time-fractional TFMDW equation [70, 76, 82] with some regularity conditions and smooth exact solutions. However, these papers ignored the presence of singularity in the solution at the initial time $t = 0$. The existing finite difference methods for the discretization of time-fractional derivatives of order $\beta \in (0,1)$ and $\alpha \in (1,2)$ are studied on uniform meshes, but some research works are there to tackle the weak singularity for Caputo derivative of order $\beta \in (0,1)$ only (see [108] related are in this). To tackle the singularity in both derivatives together of order $\beta \in (0,1)$ and $\alpha \in (1,2)$ remains to be marked. Our main interest in this work is to handle the weak initial singularity in the solution of the nonlinear time-fractional TFMDW equation. We consider the nonuniform mesh in time and uniform mesh in space direction for the discretization of the problem (3.1)-(3.3).

Contribution and purpose of proposed work

- The proposed work consists of an efficient approximation method namely nonuniform $L1$ approach to discretize the time-fractional derivatives of order $\beta \in (0,1)$ and $\alpha \in (1,2)$ at grid point t_n. We obtain the single step discretization of wave term.

- We establish and analyze a finite difference scheme based on two step ADI approach using nonuniform $L1$ method and central difference operator together to solve the 2D nonlinear TFMDW equation. We considered two type functions Klein-Gordon and Sine-Gordon for the nonlinear term $F(u)$ in the considered model (3.1).

- With some regularity conditions on the solution of nonlinear TFMDW equation and weak restrictions on mesh points, the nonuniform $L1$ difference scheme attains convergence order $\mathcal{O}(N^{-\min(2-\beta,\ 3-\alpha,\ \gamma\beta,\ \gamma(\alpha-1))} + h_1^2 + h_2^2)$.

- To illustrate the advantage of nonuniform difference scheme, we present few numerical experiments for non-smooth exact solutions along with non-zero boundary conditions with weak singularity at $t = 0$.

- We display error plots to quantify the solution layer at $t = 0$ and the impact of general mesh on computed solutions of the considered problem.

The outline of the chapter is arranged as follows: In Section 3.2, we discuss the nonuniform $L1$ method to approximate the TFCDs and prove the bound for local truncation error which appears in approximation of derivatives. A linearized finite $L1$ difference scheme based on two-step ADI approach for the governing problem (3.1)-(3.3) having singularity at $t = 0$ in the exact solution is derived in Section 3.3. We analyze the unconditional stability analysis of this scheme in Section 3.4. We present some numerical experiments with smooth and nonsmooth exact solutions to

verify the theoretical convergence rate in Section 3.5. A brief conclusion of the work is discussed in Section 3.6.

3.2 Nonuniform $L1$ Formula for Approximation of the Time-Fractional Caputo Derivatives of Order $\beta \in (0,1)$ and $\alpha \in (1,2)$

Let $0 = t_0 < t_1 < ... < t_{n-1} < t_n < ... < t_N = T$ be a nonuniform (general mesh) partition of the time interval $[0,T]$ with the grid-size $\tau_n = t_n - t_{n-1}$, $1 \le n \le N$. Throughout the chapter, we use the node points $t_k = (k\tau)^\gamma$, $0 \le k \le n$ for $\gamma \ge 1$ is a mesh grading parameter, where $\tau = T^{\frac{1}{\gamma}}/N$, and N is a positive integer. Define fractional time grid points $t_{n-\theta} = \theta t_{n-1} + (1-\theta)t_n$, for any $\theta \in [0,1]$, $n \ge 1$ and $\mathcal{U} = \{u(t_n) = u^n |\ 1 \le n \le N\}$. For $u \in \mathcal{U}$, we introduce the following notations:

$$u^{n-\frac{1}{2}} = \frac{u^n + u^{n-1}}{2}, \qquad \delta_t u^{n-\frac{1}{2}} = \frac{u^n - u^{n-1}}{\tau_n},$$
$$\delta_t^2 u^{n-\frac{1}{2}} = \frac{2}{\tau_n}\left[\frac{(u^{n+\frac{1}{2}} - u^{n-\frac{1}{2}})}{(\tau_{n+1}+\tau_n)} - \frac{(u^{n-\frac{1}{2}} - u^{n-\frac{3}{2}})}{(\tau_n + \tau_{n-1})}\right].$$

Throughout this manuscript, we suppose that the solution of problem (3.1) satisfies the following condition [108]:

$$\left|\frac{\partial^{\mathfrak{m}} u}{\partial t^{\mathfrak{m}}}(x,y,t)\right| \le C(1+t^{\alpha-\mathfrak{m}}), \quad \mathfrak{m} = 0,1,2,3, \quad \forall (x,y,t) \in \overline{\Omega} \times (0,T]. \tag{3.7}$$

(M) Considered mesh satisfy the condition $\tau_n \le c_\gamma \tau \min\left\{1, t_n^{1-\frac{1}{\gamma}}\right\}$, $1 \le n \le N$, $c_\gamma > 0$ is a constant, with $t_n \le c_\gamma t_{n-1}$ and $\frac{\tau_n}{t_n} \le c_\gamma \frac{\tau_{n-1}}{t_{n-1}}$ for $2 \le n \le N$, where $\tau = \max\limits_{1\le n\le N}\{\tau_n\}$.

We approximate the TFCDs discussed in (3.4) and (3.5) at the grid point $t = t_n$ by using the following half step length on discretized domain. For simplicity, we ignore the space variables. Let, $v(t) = \frac{\partial u(t)}{\partial t}$, then we have

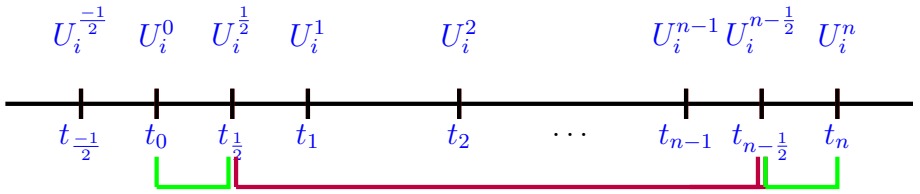

$$
\begin{aligned}
{}^{C}\mathcal{D}^m_{0,t}u(t)|_{t=t_n} = \frac{1}{\Gamma(m-\alpha)}\Bigg[& \int_{t_{n-\frac{1}{2}}}^{t_n} (t_n - s)^{m-\alpha-1}\frac{\partial^m u(s)}{\partial s^m}ds \\
& + \sum_{k=0}^{n-1}\left\{ \int_{t_{k-\frac{1}{2}}}^{t_{k+\frac{1}{2}}} (t_n - s)^{m-\alpha-1}\frac{\partial^m u(s)}{\partial s^m}ds \right\} \\
& - \int_{t_{-\frac{1}{2}}}^{t_0} (t_n - s)^{m-\alpha-1}\frac{\partial^m u(s)}{\partial s^m}ds \Bigg], \ m-1 < \alpha < m, \ m \in \mathbb{N}. \qquad (3.8)
\end{aligned}
$$

For $m = 1$ and $m = 2$, we get TFCDs defined in equations (3.4) and (3.5), respectively on the non-uniformly discretized time domain.

- For $m = 1$, we use linear interpolation polynomials for discretization of (3.8) by using the points $\{(t_{n-\frac{1}{2}}, u^{n-\frac{1}{2}}),\ (t_n, u^n)\}$, $n \geq 1$ and $(t_{k-\frac{1}{2}}, u^{k-\frac{1}{2}}),\ (t_{k+\frac{1}{2}}, u^{k+\frac{1}{2}})$, $(0 \leq k \leq n-1)$ on first and second integration, respectively and let $t_{-\frac{1}{2}} = t_0$.

- For $m = 2$, the linear interpolation polynomials are generated by utilizing the points $\{(t_{n-\frac{3}{2}}, v^{n-\frac{3}{2}}),\ (t_{n-\frac{1}{2}}, v^{n-\frac{1}{2}})\}$, $n \geq 1$ and $\{(t_{k-\frac{1}{2}}, v^{k-\frac{1}{2}}),\ (t_{k+\frac{1}{2}}, v^{k+\frac{1}{2}})\}$, $(0 \leq k \leq n-1)$ on the first and second integration of equation (3.8), respectively and let $t_{-\frac{1}{2}} = t_0$, where $v(t) = u_t(t)$. Then we get

$$
v(t_{-\frac{1}{2}}) = \frac{\partial u}{\partial t}\Big|_{t_{-\frac{1}{2}}} + \mathcal{O}(\tau_n^2) \implies v(t_0) + \mathcal{O}(\tau_n^2).
$$

Now, the nonuniform $L1$ formulas for the approximation of the TFCDs defined in (3.8) with $m = 1$ and $m = 2$ are given as follows:

$$
\begin{aligned}
&{}^{C}\mathcal{D}^{\beta}_{0,t}u(t)|_{t=t_n} \\
&\approx \frac{1}{\Gamma(1-\beta)}\Bigg[\frac{u^{n}-u^{n-\frac{1}{2}}}{t_n-t_{n-\frac{1}{2}}}\int_{t_{n-\frac{1}{2}}}^{t_n}(t_n-s)^{-\beta}ds \\
&+\sum_{k=0}^{n-1}\left(\frac{u^{k+\frac{1}{2}}-u^{k-\frac{1}{2}}}{t_{k+\frac{1}{2}}-t_{k-\frac{1}{2}}}\right)\int_{t_{k-\frac{1}{2}}}^{t_{k+\frac{1}{2}}}(t_n-s)^{-\beta}\,ds\Bigg], \qquad (3.9)\\
&=\frac{1}{\Gamma(2-\beta)}\Bigg[\frac{\tau_n^{-\beta}}{2^{1-\beta}}(u^{n}-u^{n-1}) \\
&+\sum_{k=0}^{n-1}\left\{\frac{(t_n-t_{k-\frac{1}{2}})^{1-\beta}-(t_n-t_{k+\frac{1}{2}})^{1-\beta}}{\tau_{k+1}+\tau_k}\right\}(u^{k+1}-u^{k-1})\Bigg], \qquad (3.10)\\
&=W(n)(u^{n}-u^{n-1})+\sum_{k=0}^{n-1}A_{n-k}(u^{k+1}-u^{k-1}), \qquad (3.11)
\end{aligned}
$$

$$
\begin{aligned}
&{}^{C}\mathcal{D}^{\alpha}_{0,t}u(t)|_{t=t_n} \\
&\approx \frac{2}{\Gamma(2-\alpha)}\Bigg[\frac{v^{n-\frac{1}{2}}-v^{n-\frac{3}{2}}}{\tau_{n-1}+\tau_n}\int_{t_{n-\frac{1}{2}}}^{t_n}(t_n-s)^{1-\alpha}\,ds \\
&+\sum_{k=0}^{n-1}\frac{v^{k+\frac{1}{2}}-v^{k-\frac{1}{2}}}{\tau_k+\tau_{k+1}}\int_{t_{k-\frac{1}{2}}}^{t_{k+\frac{1}{2}}}(t_n-s)^{1-\alpha}\,ds\Bigg], \qquad (3.12)\\
&=\frac{2}{\Gamma(3-\alpha)}\Bigg[\frac{1}{2^{2-\alpha}}\frac{\tau_n^{2-\alpha}}{\tau_n+\tau_{n-1}}\left\{\frac{u^{n}-u^{n-1}}{\tau_n}-\frac{u^{n-1}-u^{n-2}}{\tau_{n-1}}\right\} \\
&+\sum_{k=0}^{n-1}\left\{\frac{(t_n-t_{k-\frac{1}{2}})^{2-\alpha}-(t_n-t_{k+\frac{1}{2}})^{2-\alpha}}{\tau_{k+1}+\tau_k}\right\}\left\{\frac{u^{k+1}-u^{k}}{\tau_{k+1}}-\frac{u^{k}-u^{k-1}}{\tau_k}\right\}\Bigg], \\
&=Z(n)\left\{\frac{u^{n}-u^{n-1}}{\tau_n}-\frac{u^{n-1}-u^{n-2}}{\tau_{n-1}}\right\}+\sum_{k=0}^{n-1}B_{n-k}\left\{\frac{u^{k+1}-u^{k}}{\tau_{k+1}}-\frac{u^{k}-u^{k-1}}{\tau_k}\right\}, \qquad (3.13)
\end{aligned}
$$

where, corresponding coefficients of equations (3.11) and (3.13) are defined as:

$$W(n)=\frac{1}{\Gamma(2-\beta)}\frac{\tau_n^{-\beta}}{2^{1-\beta}},\quad A_{n-k}=\frac{1}{\Gamma(2-\beta)}\frac{(t_n-t_{k-\frac{1}{2}})^{1-\beta}-(t_n-t_{k+\frac{1}{2}})^{1-\beta}}{\tau_{k+1}+\tau_k}, \tag{3.14}$$

$$Z(n)=\frac{2^{\alpha-1}}{\Gamma(3-\alpha)}\frac{\tau_n^{2-\alpha}}{\tau_n+\tau_{n-1}},\quad B_{n-k}=\frac{2}{\Gamma(3-\alpha)}\frac{(t_n-t_{k-\frac{1}{2}})^{2-\alpha}-(t_n-t_{k+\frac{1}{2}})^{2-\alpha}}{\tau_{k+1}+\tau_k}. \tag{3.15}$$

By using the mean value theorem, we can easily prove that

$$0<A_{n-k+1}\le A_{n-k},\quad 0<B_{n-k+1}\le B_{n-k},\ W(n)\ge 0,\ Z(n)\ge 0,\quad \forall n\ge 1. \tag{3.16}$$

The following inequality will be helpful in proving the error bound

$$\begin{aligned}\tau_n :&= T\left[\left(\frac{n}{N}\right)^{\gamma}-\left(\frac{n-1}{N}\right)^{\gamma}\right]=TN^{-\gamma}[n^{\gamma}-(n-1)^{\gamma}],\\ &=TN^{-\gamma}n^{\gamma}\left[1-\left(1-1/n\right)^{\gamma}\right]\le CTN^{-\gamma}n^{\gamma-1}.\end{aligned} \tag{3.17}$$

3.2.1 Local Truncation Error for TFCDs Term

Lemma 3.2.1. Suppose $0<\beta<1$, $n\in\{1,2,...,N\}$ and $u\in C^2[0,T]\cap C^3(0,T]$. From equation (3.9), it holds that

$$r_k^n=\frac{1}{\Gamma(1-\beta)}\sum_{k=0}^{n-1}\int_{t_{k-\frac{1}{2}}}^{t_{k+\frac{1}{2}}}(t_n-s)^{-\beta}\left[u'(s)-\frac{u^{k+\frac{1}{2}}-u^{k-\frac{1}{2}}}{t_{k+\frac{1}{2}}-t_{k-\frac{1}{2}}}\right]ds, 0\le k\le n-2, \tag{3.18}$$

$$r_n^n=\frac{1}{\Gamma(1-\beta)}\int_{t_{n-\frac{1}{2}}}^{t_n}(t_n-s)^{-\beta}\left[u'(s)-\frac{u^n-u^{n-\frac{1}{2}}}{t_n-t_{n-\frac{1}{2}}}\right]ds,\quad 1\le n\le N, \tag{3.19}$$

where

$$|r_k^n| \leq \widehat{C}_1\ n^{-\min\{2-\beta,\ \gamma\beta\}}, \qquad |r_n^n| \leq \widehat{C}_2\ n^{-\min\{2-\beta,\ \gamma\beta\}}. \tag{3.20}$$

Proof. By Taylor theorem, $t_{k-\frac{1}{2}} < t < t_{k+\frac{1}{2}}$, then

$$u'(t) - \frac{u^{k+1}-u^{k-1}}{t_{k+1}-t_{k-1}} = \frac{1}{\tau_{k+1}+\tau_k}\left[\left\{\int_{t_{k-\frac{1}{2}}}^{t}(\eta - t_{k-\frac{1}{2}}) - \int_{t}^{t_{k+\frac{1}{2}}}(t_{k+\frac{1}{2}}-\eta)\right\}u''(\eta)d\eta\right]. \tag{3.21}$$

From equations (3.18) and (3.21), we get

$$\begin{aligned}
|r_k^n| &= \left|\frac{1}{\Gamma(1-\beta)}\left\{\sum_{k=1}^{n-2}\frac{1}{\tau_{k+1}+\tau_k}\int_{t_{k-\frac{1}{2}}}^{t_{k+\frac{1}{2}}}\left[\int_{t_{k-\frac{1}{2}}}^{s}(\eta - t_{k-\frac{1}{2}})u''(\eta)d\eta\right.\right.\right.\\
&\left.\left.\left.- \int_{s}^{t_{k+\frac{1}{2}}}(t_{k+\frac{1}{2}}-\eta)u''(\eta)d\eta\right](t_n-s)^{-\beta}ds\right\}\right|\\
&= \left|\frac{1}{\Gamma(1-\beta)}\left\{\sum_{k=1}^{n-2}\frac{1}{\tau_{k+1}+\tau_k}\int_{t_{k-\frac{1}{2}}}^{t_{k+\frac{1}{2}}}\left[\left(\int_{\eta}^{t_{k+\frac{1}{2}}}(t_n-s)^{-\beta}ds\right)(\eta - t_{k-\frac{1}{2}})\right.\right.\right.\\
&\left.\left.\left.- \left(\int_{t_{k-\frac{1}{2}}}^{\eta}(t_n-s)^{-\beta}ds\right)(t_{k+\frac{1}{2}}-\eta)\right]\right\}u''(\eta)d\eta\right|\\
&= \left|\frac{1}{\Gamma(2-\beta)}\sum_{k=1}^{n-2}\frac{1}{\tau_{k+1}+\tau_k}\int_{t_{k-\frac{1}{2}}}^{t_{k+\frac{1}{2}}}\left[(\eta - t_{k-\frac{1}{2}})\{(t_n-\eta)^{1-\beta} - (t_n - t_{k+\frac{1}{2}})^{1-\beta}\}\right.\right.\\
&\left.\left.- (t_{k+\frac{1}{2}}-\eta)\{(t_n-t_{k-\frac{1}{2}})^{1-\beta} - (t_n-\eta)^{1-\beta}\}\right]u''(\eta)d\eta\right|\\
&\leq \frac{2^{\beta-3}}{\Gamma(2-\beta)}\left|\sum_{k=1}^{n-2}\left[\frac{[(2t_n - t_{k+1}-t_k)^{2-\beta} - (2t_n - t_k - t_{k-1})^{2-\beta}]}{(2-\beta)} - \frac{\tau_{k+1}+\tau_k}{2}\right.\right.\\
&\qquad\left.\left.[(2t_n - t_k - t_{k-1})^{1-\beta} + (2t_n - t_{k+1}-t_k)^{1-\beta}]\right]\right| \max_{t_0\leq\xi_1\leq t_n}|u''(\xi_1)|.
\end{aligned} \tag{3.22}$$

Since $t_k = T(\frac{k}{N})^\gamma$, $\gamma \geq 1$ and $t_n - t_k = \frac{\tau_n+\tau_{k+1}}{2}\ (n-k)$, therefore

$$\begin{aligned}
(2t_n - t_{k+1} - t_k)^{2-\beta} &= \left[\frac{\tau_n+\tau_{k+2}}{2}(n-k-1) + \frac{\tau_n+\tau_{k+1}}{2}(n-k)\right]^{2-\beta}\\
&\leq \tau_n^{2-\beta}[2(n-k)-1]^{2-\beta}.
\end{aligned} \tag{3.23}$$

We solve summation term of equation (3.22) in two parts. For $1 \leq k \leq \lceil \frac{n}{2} \rceil - 1$, we get

$$[2n^{\gamma} - (k+1)^{\gamma} - k^{\gamma}]^{2-\beta} N^{-\gamma(2-\beta)} T^{2-\beta} \leq C N^{-\gamma(2-\beta)} n^{\{(\gamma-1)(2-\beta)\}} T^{2-\beta} [2(n-k)-1]^{2-\beta}.$$

Then first term of summation in (3.22) has following bound

$$\begin{aligned}
&\left|(2t_n - t_{k+1} - t_k)^{2-\beta} - (2t_n - t_k - t_{k-1})^{2-\beta}\right| \\
&\leq (2t_n - t_{k+1} - t_k)^{2-\beta} + (2t_n - t_k - t_{k-1})^{2-\beta} \\
&\leq C N^{-\gamma(2-\beta)} n^{\{(\gamma-1)(2-\beta)\}} T^{2-\beta} \{[2(n-k)-1]^{2-\beta} + [2(n-k)+1]^{2-\beta}\}, \qquad (3.24)
\end{aligned}$$

and bound for the second term in the summation (3.22) is:

$$\begin{aligned}
&|(2t_n - t_k - t_{k-1})^{1-\beta} + (2t_n - t_{k+1} - t_k)^{1-\beta}| \\
&\leq C N^{-\gamma(1-\beta)} n^{\{(\gamma-1)(1-\beta)\}} T^{1-\beta} \{[2(n-k)+1]^{1-\beta} + [2(n-k)-1]^{1-\beta}\}, \qquad (3.25)
\end{aligned}$$

Now applying summation on (3.25), we get

$$\begin{aligned}
&\left| \sum_{k=1}^{\lceil \frac{n}{2} \rceil - 1} \frac{\tau_{k+1} + \tau_k}{2} \left[(2t_n - t_k - t_{k-1})^{1-\beta} + (2t_n - t_{k+1} - t_k)^{1-\beta}\right] \right| \\
&\leq C N^{-\gamma(2-\beta)} n^{\{(\gamma-1)(1-\beta)\}} T^{2-\beta} \sum_{k=1}^{\lceil \frac{n}{2} \rceil - 1} \left| \left[(n^{\gamma} - (k-1)^{\gamma})^{1-\beta} + (n^{\gamma} - k^{\gamma})^{1-\beta}\right] \right| \\
&\leq C N^{-\gamma(2-\beta)} n^{\{(\gamma-1)(1-\beta)\}} T^{2-\beta} \sum_{k=1}^{\lceil \frac{n}{2} \rceil - 1} (n^{\gamma} - (k-1)^{\gamma})^{1-\beta} \\
&\leq C N^{-\gamma(2-\beta)} T^{2-\beta} n^{\{(\gamma-1)(2-\beta)\}}. \qquad (3.26)
\end{aligned}$$

Now, we combine the equations (3.24) and (3.26) to get error bound for the case $1 \leq k \leq \lceil \frac{n}{2} \rceil - 1$

$$|r_k^n| \leq CN^{-\gamma(2-\beta)}T^{2-\beta}n^{\{(\gamma-1)(2-\beta)\}} \max_{\widehat{\eta}_1 \in [t_{k-\frac{1}{2}}, t_{k+\frac{1}{2}}]} |u''(\widehat{\eta}_1)|, \tag{3.27}$$

and the inequality $|\frac{\partial^2 u(t)}{\partial t^2}| \leq C(1+t^{\beta-2})$ handles the maximum value of second order derivative of u in above equation (3.27). For $\lceil \frac{n}{2} \rceil \leq k \leq n-1$,

$$\begin{aligned}
|r_k^n| &= \left| \frac{1}{\Gamma(2-\beta)} \sum_{k=\lceil \frac{n}{2} \rceil}^{n-2} \frac{1}{\tau_{k+1}+\tau_k} \int_{t_{k-\frac{1}{2}}}^{t_{k+\frac{1}{2}}} \Big[(\eta - t_{k-\frac{1}{2}})\{(t_n - \eta)^{1-\beta} - (t_n - t_{k+\frac{1}{2}})^{1-\beta}\} \right. \\
&\qquad \left. - (t_{k+\frac{1}{2}} - \eta)\{(t_n - t_{k-\frac{1}{2}})^{1-\beta} - (t_n - \eta)^{1-\beta}\} \Big] u''(\eta) d\eta \right| \\
&\leq \left| \frac{C}{\tau_{k+1}+\tau_k} \left[\int_{t_{\lceil \frac{n}{2} \rceil - \frac{1}{2}}}^{t_{n-\frac{3}{2}}} (\eta - t_{k-\frac{1}{2}})(t_n - \eta)^{1-\beta} d\eta \right. \right. \\
&\qquad \left. \left. + \int_{t_{\lceil \frac{n}{2} \rceil - \frac{1}{2}}}^{t_{n-\frac{3}{2}}} (t_{k+\frac{1}{2}} - \eta)(t_n - \eta)^{1-\beta} d\eta \right] \right| \max_{\widehat{\eta}_2 \in [t_{k-\frac{1}{2}}, t_{k+\frac{1}{2}}]} |u''(\widehat{\eta}_2)| \\
&\leq \left| \frac{C}{\tau_{k+1}+\tau_k} (t_{k+\frac{1}{2}} - t_{k-\frac{1}{2}}) \left[(t_n - t_{\lceil \frac{n}{2} \rceil - \frac{1}{2}})^{2-\beta} \right] \right| \max_{\widehat{\eta}_2 \in [t_{k-\frac{1}{2}}, t_{k+\frac{1}{2}}]} |u''(\widehat{\eta}_2)|.
\end{aligned} \tag{3.28}$$

In equation (3.18), it remains to show bound for $k = 0$ and $k = n-1$. For $n = 1$, $k = 0$, then

$$\begin{aligned}
|r_0^1| &= \left| \frac{1}{\Gamma(1-\beta)} \int_{t_0}^{t_{\frac{1}{2}}} (t_1 - s)^{-\beta} \left[\frac{\partial u(s)}{\partial s} - \frac{u^{\frac{1}{2}} - u^0}{t_{\frac{1}{2}} - t_0} \right] ds \right| \\
&\leq \left| \frac{1}{\Gamma(1-\beta)} \left[\int_{t_0}^{t_{\frac{1}{2}}} (t_1 - s)^{-\beta} \frac{\partial u(s)}{\partial s} ds - (t_1 - t_{\frac{1}{2}})^{-\beta} \int_{t_0}^{t_{\frac{1}{2}}} \frac{\partial u(s)}{\partial s} ds \right] \right| \\
&\leq \frac{C}{\Gamma(1-\beta)} \left[\int_{t_0}^{t_{\frac{1}{2}}} (t_1 - s)^{-\beta} s^{\beta-1} ds - \frac{1}{\beta} \right] \\
&\leq \frac{C}{\Gamma(1-\beta)} \left[(t_1 - t_{\frac{1}{2}})^{-\beta} \left[\frac{s^\beta}{\beta} \right]_{t_0}^{t_{\frac{1}{2}}} - \frac{1}{\beta} \right] \\
&\leq \frac{C}{\Gamma(1-\beta)} \left[\frac{1}{\beta} \left(\frac{t_1 - t_{\frac{1}{2}}}{t_{\frac{1}{2}}} \right)^{-\beta} - \frac{1}{\beta} \right] \leq C.
\end{aligned} \tag{3.29}$$

Now, suppose that $n > 1$ and $k = 0$, then the error bound

$$
\begin{aligned}
&|r_0^n| \\
&= \left| \frac{1}{\Gamma(1-\beta)} \int_{t_0}^{t_{\frac{1}{2}}} (t_n - s)^{-\beta} \left[\frac{\partial u(s)}{\partial s} - \frac{u^{\frac{1}{2}} - u^0}{t_{\frac{1}{2}} - t_0} \right] ds \right| \\
&\leq \left| \frac{C}{\Gamma(1-\beta)} \left[\frac{(t_n - t_0)^{1-\beta} - (t_n - t_{\frac{1}{2}})^{1-\beta}}{\frac{\tau_1}{2}} \int_{t_0}^{t_{\frac{1}{2}}} s^{\beta-1} ds - (t_n - t_{\frac{1}{2}})^{-\beta} \int_{t_0}^{t_{\frac{1}{2}}} s^{\beta-1} ds \right] \right| \\
&\leq \left| \frac{C}{\beta\Gamma(1-\beta)} \left[\{t_n^{1-\beta} - (t_n - t_{\frac{1}{2}})^{1-\beta}\} \, t_{\frac{1}{2}}^{\beta-1} - (t_n - t_{\frac{1}{2}})^{-\beta} \, t_{\frac{1}{2}}^{\beta} \right] \right| \\
&\leq \frac{C}{\beta\Gamma(1-\beta)} \left[\frac{t_n - t_{\frac{1}{2}}}{t_{\frac{1}{2}}} \right]^{-\beta} \\
&\leq Cn^{-\gamma\beta}. \qquad (3.30)
\end{aligned}
$$

Now, we consider the case $k = n - 1$. From equation (3.18), for some $\eta_1,\ \eta_2,\ \eta_3 \in (t_{n-\frac{3}{2}}, t_{n-\frac{1}{2}})$

$$
\begin{aligned}
|r_{n-1}^n| &= \frac{1}{\Gamma(1-\beta)} \left| \frac{\partial u(\eta_1)}{\partial t} - \frac{\partial u(\eta_2)}{\partial t} \right| \int_{t_{n-\frac{3}{2}}}^{t_{n-\frac{1}{2}}} (t_n - s)^{-\beta} ds \\
&\leq \frac{\tau_n}{\Gamma(2-\beta)} \max_{\eta_3 \in [t_{n-\frac{3}{2}} t_{n-\frac{1}{2}}]} |u''(\eta_3)| \, (t_n - t_{n-\frac{3}{2}})^{1-\beta} \\
&\leq C \, t_{n-1}^{\beta-2} \, \tau_n^{2-\beta} \\
&\leq CN^{-\gamma(\beta-2)} T^{2-\beta} (n^\gamma - (n-1)^\gamma)^{2-\beta} T^{\beta-2} N^{\gamma(\beta-2)} (n-1)^{\gamma(2-\beta)} \\
&\leq C(n-1)^{(\gamma-1)(2-\beta)} (n-1)^{\gamma(\beta-2)} \\
&\leq Cn^{-(2-\beta)}. \qquad (3.31)
\end{aligned}
$$

Now, using equation (3.21) in (3.19), we get error bound on $[t_{n-\frac{1}{2}}, t_n]$

$$
\begin{aligned}
|r_n^n| \leq \Bigg| \frac{1}{\Gamma(1-\beta)\tau_n} \int_{t_{n-\frac{1}{2}}}^{t_n} \Bigg[\int_{t_{n-\frac{1}{2}}}^{s} (\eta - t_{n-\frac{1}{2}}) u''(\eta) d\eta \\
- \int_s^{t_n} (t_n - \eta) u''(\eta) d\eta \Bigg] (t_n - s)^{-\beta} ds \Bigg|
\end{aligned}
$$

$$
\begin{aligned}
&\leq |\frac{\tau_n^{-1}}{2\Gamma(1-\beta)}\Big[\int_{t_{n-\frac{1}{2}}}^{t_n}(s-t_{n-\frac{1}{2}})^2(t_n-s)^{-\beta}ds \\
&-\int_{t_{n-\frac{1}{2}}}^{t_n}(t_n-s)^{2-\beta}ds\Big]\max_{\widehat{\eta}_3\in[t_{n-\frac{1}{2}},t_n]}|u''(\widehat{\eta}_3)| \\
&\leq \Big|\frac{\tau_n^{-1}}{2\Gamma(1-\beta)}\ t_n^{\beta-2}\ \int_{t_{n-\frac{1}{2}}}^{t_n}(s-t_{n-\frac{1}{2}})^2(t_n-s)^{-\beta}ds\Big| \\
&= \frac{\tau_n^{-1}}{\Gamma(4-\beta)}\ t_n^{\beta-2}\ (t_n-t_{n-\frac{1}{2}})^{3-\beta} \\
&\leq C\ \tau_n^{2-\beta}\ t_n^{\beta-2} \\
&\leq CT^{2-\beta}N^{-\gamma(2-\beta)}n^{(\gamma-1)(2-\beta)}T^{\beta-2}N^{-\gamma(\beta-2)}n^{\gamma(\beta-2)} \\
&\leq Cn^{-(2-\beta)}. \qquad (3.32)
\end{aligned}
$$

□

Lemma 3.2.2. Suppose $1<\alpha<2$, $n\in\{1,2,...,N\}$ and $u\in C^2[0,T]\cap C^3(0,T]$. Then by using (3.12), it holds that

$$\mathcal{R}_1^n=\frac{1}{\Gamma(2-\alpha)}\sum_{k=0}^{n-1}\int_{t_{k-\frac{1}{2}}}^{t_{k+\frac{1}{2}}}(t_n-s)^{1-\alpha}\Big[v'(s)-\frac{v^{k+\frac{1}{2}}-v^{k-\frac{1}{2}}}{t_{k+\frac{1}{2}}-t_{k-\frac{1}{2}}}\Big]ds, \qquad (3.33)$$

$$\mathcal{R}_2^n=\frac{1}{\Gamma(2-\alpha)}\int_{t_{n-\frac{1}{2}}}^{t_n}(t_n-s)^{1-\alpha}\Big[v'(s)-\frac{v^{n-\frac{1}{2}}-v^{n-\frac{3}{2}}}{t_{n-\frac{1}{2}}-t_{n-\frac{3}{2}}}\Big]ds, \qquad (3.34)$$

where

$$|\mathcal{R}_k^n|\leq\widetilde{C}_1\ n^{-\min\{3-\alpha,\ \gamma(\alpha-1)\}},\qquad |\mathcal{R}_n^n|\leq\widetilde{C}_2\ n^{-\min\{3-\alpha,\ \gamma(\alpha-1)\}}. \qquad (3.35)$$

Proof. We prove this Lemma by using similar idea as in Lemma 3.2.1. □

By using the formulas (3.11) and (3.13), we can express the approximation of the sum of the both operators ${}^C\mathcal{D}_{0,t}^{\beta}$ and ${}^C\mathcal{D}_{0,t}^{\alpha}$. Then, we get the following compact

form

$$
\begin{aligned}
&{}^{C}\mathcal{D}^{\beta}_{0,t}u(t_n) + {}^{C}\mathcal{D}^{\alpha}_{0,t}u(t_n)\\
&= W(n)(u^n - u^{n-1}) + Z(n)\left\{\frac{u^n - u^{n-1}}{\tau_n} - \frac{u^{n-1} - u^{n-2}}{\tau_{n-1}}\right\}\\
&+ \sum_{k=0}^{n-1} A_{n-k}(u^{k+1} - u^{k-1}) + \sum_{k=0}^{n-1} B_{n-k}\left\{\frac{u^{k+1} - u^k}{\tau_{k+1}} - \frac{u^k - u^{k-1}}{\tau_k}\right\} + \mathbb{E}^n, \quad n \geq 1,\\
&= W(n)(u^n - u^{n-1}) + Z(n)\left\{\frac{u^n - u^{n-1}}{\tau_n} - \frac{u^{n-1} - u^{n-2}}{\tau_{n-1}}\right\} + \left(A_1 + \frac{B_1}{\tau_n}\right)(u^n - u^{n-1})\\
&+ \sum_{k=1}^{n-1}\left\{(A_{n-k+1} + A_{n-k}) + \frac{B_{n-k+1} - B_{n-k}}{\tau_k}\right\}(u^k - u^{k-1}) - B_n\delta_t u(t_0) + \mathbb{E}^n,\\
&= \left[W(n) + A_1 + \frac{Z(n) + B_1}{\tau_n}\right](u^n - u^{n-1}) - \frac{Z(n)}{\tau_{n-1}}(u^{n-1} - u^{n-2})\\
&\quad + \sum_{k=1}^{n-1}\Lambda_{n-k}(u^k - u^{k-1}) - B_n\delta_t u^0 + \mathbb{E}^n, \qquad n \geq 2.
\end{aligned}
\tag{3.36}
$$

Where coefficients $W(n)$, $Z(n)$, A_{n-k} and B_{n-k} are defined in equations (3.14) and (3.15). Then the corresponding coefficients of (3.36) are given as:

$$
\Lambda_{n-k} = \begin{cases} (A_n + A_{n-1}) + \frac{B_n - B_{n-1}}{\tau_1}, & k = 1,\\ (A_{n-k+1} + A_{n-k}) + \frac{B_{n-k+1} - B_{n-k}}{\tau_k}, & 2 \leq k \leq n-2,\\ (A_2 + A_1) + \frac{B_2 - B_1}{\tau_{n-1}}, & k = n-1. \end{cases}
\tag{3.37}
$$

For $n = 1$,

$$
{}^{C}\mathcal{D}^{\beta}_{0,t}u(t_n) + {}^{C}\mathcal{D}^{\alpha}_{0,t}u(t_n) = \left[W(1) + A_1 + \frac{Z(1) + B_1}{\tau_1}\right](u^1 - u^0) - B_1\delta_t u^0 + \mathbb{E}^1,
\tag{3.38}
$$

where truncation error is $\mathbb{E}^n = r_1^n + r_2^n + \mathcal{R}_1^n + \mathcal{R}_2^n$. Then $|\mathbb{E}^n| \leq \widehat{C}N^{-\min(2-\beta,\ 3-\alpha,\gamma\beta,\gamma(\alpha-1))}$. Using the inequalities of equation (3.16) and mean value theorem, we can easily prove

that

$$\Lambda_{n-k+1} \leq \Lambda_{n-k}, \quad 1 \leq k \leq n-1. \tag{3.39}$$

3.3 Methodology for Nonuniform $L1$ Difference Scheme

Now, we discuss both one-dimensional and two-dimensional numerical difference schemes on nonuniform temporal meshes for the considered problem (3.1).

3.3.1 The One-Dimensional Scheme

Let $h = \frac{L}{M}$ be the step-size for the space variable and $\omega_s = \{x_i = ih | 1 \leq i \leq M-1\}$ be the space domain with boundary $\overline{\omega}_s = \omega_s \cup \partial\omega_s$. Then equation (3.1) at the grid point (x_i, t_n) is defined as:

$$\begin{cases} {}^{C}\mathcal{D}^{\beta}_{0,t} u(x_i,t_n) + {}^{C}\mathcal{D}^{\alpha}_{0,t} u(x_i,t_n) + F(u(x_i,t_n)) \\ \qquad = \frac{\partial^2 u(x_i,t_n)}{\partial x^2} + f(x_i,t_n), \ x_i \in \omega_s, 1 \leq n \leq N, \\ u(x_i,0) = \phi(x_i), \quad \frac{\partial u(x_i,0)}{\partial t} = \varphi(x_i), \quad 1 \leq i \leq M-1, \\ u(x_i,t_n) = \Phi(x_i,t_n), \quad i \in \{0, M\}, \quad 1 \leq n \leq N. \end{cases} \tag{3.40}$$

To approximate the Caputo derivatives on left-hand side of equation (3.40), we use formula (3.36), and central difference approximation to discretize the spatial

derivative on right-hand side of equation (3.40), we get

$$\begin{aligned}\left[W(n)+A_1+\frac{Z(n)+B_1}{\tau_n}\right](u_i^n-u_i^{n-1})-\frac{Z(n)}{\tau_{n-1}}(u_i^{n-1}-u_i^{n-2})\\ +\sum_{k=1}^{n-1}\Lambda_{n-k}(u_i^k-u_i^{k-1})+F(u_i^n)-B_n\varphi_i\\ =\frac{1}{h^2}(u_{i+1}^n-2u_i^n+u_{i-1}^n)+f_i^n+\mathcal{R}_i^n,\quad x_i\in\omega_s,\ 1\le n\le N.\end{aligned}\tag{3.41}$$

Denote

$$W(n)+A_1+\frac{Z(n)+B_1}{\tau_n}=\mathfrak{I}_n,\qquad 1\le n\le N,\tag{3.42}$$

$$F(u_i^n)=F(u_i^{n-1})+(u_i^n-u_i^{n-1})\partial_u F(u_i^{n-1}):=\widetilde{F}(u_i^{n-1}),\quad 1\le n\le N.\tag{3.43}$$

Now, we obtain the linearized implicit difference scheme from equation (3.41) as:

$$\begin{aligned}-\frac{1}{h^2}u_{i-1}^n+\left[\mathfrak{I}_n+\frac{2}{h^2}\right]u_i^n-\frac{1}{h^2}u_{i+1}^n=\left[\mathfrak{I}_n+\frac{Z(n)}{\tau_{n-1}}\right]u_i^{n-1}-\frac{Z(n)}{\tau_{n-1}}u_i^{n-2}\\ -\sum_{k=1}^{n-1}\Lambda_{n-k}(u_i^k-u_i^{k-1})-\widetilde{F}(u_i^{n-1})+f_i^n+B_n\varphi_i+\mathcal{R}_i^n,\ x_i\in\omega_s,\ 1\le n\le N\end{aligned}\tag{3.44}$$

where $\mathcal{R}_i^n\le C(N^{-\gamma\min(2-\beta,\ 3-\alpha,\ \gamma\beta,\ \gamma(\alpha-1))}+h^2)$ for a positive constant C. We replace the analytical solution $u_{i,j}^n$ by its numerical solution $U_{i,j}^n$ to omit the error term in the equation (3.44). Then, we get the numerical scheme in compact form as:

$$\mathcal{L}U^n=b,$$

where

$$\begin{cases} \mathcal{L}U^n & = -\frac{1}{h^2}U_{i-1}^n + \left[\mathfrak{I}_n + \frac{2}{h^2}\right]U_i^n - \frac{1}{h^2}U_{i+1}^n \\ b & = \left[\mathfrak{I}_n + \frac{Z(n)}{\tau_{n-1}}\right]U_i^{n-1} - \frac{Z(n)}{\tau_{n-1}}U_i^{n-2} - \sum_{k=1}^{n-1}\Lambda_{n-k}(U_i^k - U_i^{k-1}) \\ & \quad - \widetilde{F}(U_i^{n-1}) + f_i^n + B_n\varphi_i, \qquad n \geq 1. \end{cases} \tag{3.45}$$

3.3.2 The Two-Dimensional Scheme

Let $h_1 = \frac{L_1}{M_1}$ and $h_2 = \frac{L_2}{M_2}$ be the step-sizes for space variables with grid points $x_i = ih_1$ and $y_j = jh_2$, respectively. The mesh points domain is $\Omega_s = \{(ih_1, jh_2)|1 \leq i \leq M_1 - 1, 1 \leq j \leq M_2 - 1\}$ with the boundary $\overline{\Omega}_s = \Omega_s \cup \partial\Omega_s$.

Then, we define the index sets

$$\mathcal{I} = \{(i,j)|1 \leq i \leq M_1 - 1,\ 1 \leq j \leq M_2 - 1\},\ \ \overline{\mathcal{I}} = \{(i,j)|0 \leq i \leq M_1,\ 0 \leq j \leq M2\}.$$

The functions at grid points $u(x_i, y_j, t_n) = u_{i,j}^n$, $f(x_i, y_j, t_n) = f_{i,j}^n$, $F(u(x_i, y_j, t_n)) = F(u_{i,j}^n)$ for $0 \leq n \leq N$, $(i,j) \in \overline{\mathcal{I}}$. Suppose the grid functions space $\mathfrak{U} = \{u(x_i, y_j, t_n) = u_{i,j}^n \mid (i,j) \in \overline{\mathcal{I}},\ 0 \leq n \leq N\}$. For $u \in \mathfrak{U}$, we define the following notations:

$$\begin{cases} \delta_x u_{i-\frac{1}{2},j}^n = \frac{u_{i,j}^n - u_{i-1,j}^n}{h_x}, \quad \delta_{xx} u_{i,j}^n = \frac{u_{i+1,j}^n - 2u_{i,j}^n + u_{i-1,j}^n}{h_x^2}, \\ \delta_y \delta_x u_{i-\frac{1}{2},j-\frac{1}{2}} = \frac{1}{h_1}(\delta_y u_{i,j-\frac{1}{2}} - \delta_y u_{i-1,j-\frac{1}{2}}), \\ \Delta_h u_{i,j} = \delta_{xx} u_{i,j} + \delta_{yy} u_{i,j}. \end{cases} \tag{3.46}$$

Similar notations used for y variable. Considered model (3.1) at the grid point (x_i, y_j, t_n) using the approximation of Caputo derivatives from the equation (3.36),

we have

$$\begin{cases} {}^{C}\mathcal{D}^{\beta}_{0,t}u(x_i,y_j,t_n) + {}^{C}\mathcal{D}^{\alpha}_{0,t}u(x_i,y_j,t_n) + F(u(x_i,y_j,t_n)) \\ = \Delta_h u(x_i,y_j,t_n) + f(x_i,y_j,t_n), \quad (i,j)\in\overline{\mathcal{I}}, \quad 1\le n\le N, \\ u(x_i,y_j,0) = \phi(x_i,y_j), \quad \frac{\partial u(x_i,y_j,0)}{\partial t} = \varphi(x_i,y_j), \quad (i,j)\in\mathcal{I}, \\ u(x_i,y_j,t_n) = \Phi(x_i,y_j,t_n), \quad (i,j)\in\partial\overline{\mathcal{I}}(\equiv\mathcal{I}\cap\overline{\mathcal{I}}), \quad 1\le n\le N. \end{cases} \tag{3.47}$$

Using equations (3.36) and (3.42) to approximate the Caputo derivatives on the left-hand side of equation (3.47) and central difference operators to approximate the space derivatives in right-hand side of equation (3.47). Then we obtain the following linearized implicit difference scheme

$$\begin{aligned} &\mathfrak{I}_n(u^n_{i,j}-u^{n-1}_{i,j}) - \frac{Z(n)}{\tau_{n-1}}(u^{n-1}_{i,j}-u^{n-2}_{i,j}) + \sum_{k=1}^{n-1}\Lambda_{n-k}(u^k_{i,j}-u^{k-1}_{i,j}) - B_n\varphi_{i,j} \\ &+ \widetilde{F}(u^{n-1}_{i,j}) = \Delta_h u^n_{i,j} + f^n_{i,j} + \mathfrak{R}^n_{i,j}, \quad (i,j)\in\mathcal{I}, \quad 1\le n\le N, \end{aligned} \tag{3.48}$$

where $|\mathfrak{R}^n_{i,j}| \le C(N^{-\min\left(2-\beta,\ 3-\alpha,\ \gamma\beta,\ \gamma(\alpha-1)\right)} + h_1^2 + h_2^2)$ and $\mathfrak{I}_n$ defined in (3.42). Let, $\mu = \mathfrak{I}_n^{-1}$, and replacing the exact solution $u^n_{i,j}$ by the approximate solution $U^n_{i,j}$ to omit the error term in (3.48), we get

$$\begin{aligned} U^n_{i,j} - \mu\Delta_h U^n_{i,j} = &\left[1+\mu\frac{Z(n)}{\tau_{n-1}}\right]U^{n-1}_{i,j} - \mu\frac{Z(n)}{\tau_{n-1}}U^{n-2}_{i,j} - \sum_{k=1}^{n-1}\mu\Lambda_{n-k}(U^k_{i,j}-U^{k-1}_{i,j}) \\ &- \mu\widetilde{F}(U^{n-1}_{i,j}) + \mu f^n_{i,j} + \mu B_n\varphi_{i,j}, \quad (i,j)\in\mathcal{I}, \quad 1\le n\le N. \end{aligned} \tag{3.49}$$

To construct the ADI scheme, we add a small term $({}^{C}\mathcal{D}^{\beta}_{0,t} + {}^{C}\mathcal{D}^{\alpha}_{0,t})\mu^2\delta_x^2\delta_y^2 U^n_{i,j}$ to equation (3.49), and obtain

$$(I-\mu\delta_x^2)(I-\mu\delta_y^2)U^n_{i,j} = \left[1+\mu\frac{Z(n)}{\tau_{n-1}}\right]\left(U^{n-1}_{i,j} + \mu^2\delta_x^2\delta_y^2 U^{n-1}_{i,j}\right) - \mu\frac{Z(n)}{\tau_{n-1}}\left(U^{n-2}_{i,j}\right.$$

$$+\mu^2\delta_x^2\delta_y^2U_{i,j}^{n-2}\big)-\mu\sum_{k=1}^{n-1}\Lambda_{n-k}\big[\big(U_{i,j}^{k}+\mu^2\delta_x^2\delta_y^2U_{i,j}^{k}\big)-\big(U_{i,j}^{k-1}+\mu^2\delta_x^2\delta_y^2U_{i,j}^{k-1}\big)\big]$$

$$-\mu\widetilde{F}(U_{i,j}^{n-1})+\mu f_{i,j}^{n}+\mu B_n\varphi_{i,j},\quad (i,j)\in\mathcal{I},\quad 1\le n\le N. \tag{3.50}$$

Suppose an intermediate variable $V_{i,j}^{*}=(I-\mu\delta_y^2)U_{i,j}^{n},\ 0\le i\le M_1,\ 1\le j\le M_2-1$. For fixed $j\in\mathcal{I}$, we first solve the following system of equations to find the intermediate solution $V_{i,j}^{*}$

$$\begin{cases}(I-\mu\delta_x^2)V_{i,j}^{*}=\big[1+\mu\frac{Z(n)}{\tau_{n-1}}\big]\big(U_{i,j}^{n-1}+\mu^2\delta_x^2\delta_y^2U_{i,j}^{n-1}\big)-\mu\frac{Z(n)}{\tau_{n-1}}\big(U_{i,j}^{n-2}\\ +\mu^2\delta_x^2\delta_y^2U_{i,j}^{n-2}\big)-\mu\sum_{k=1}^{n-1}\Lambda_{n-k}\big[\big(U_{i,j}^{k}+\mu^2\delta_x^2\delta_y^2U_{i,j}^{k}\big)-\big(U_{i,j}^{k-1}\\ +\mu^2\delta_x^2\delta_y^2U_{i,j}^{k-1}\big)\big]-\mu\widetilde{F}(U_{i,j}^{n-1})+\mu f_{i,j}^{n}+\mu B_n\varphi_{i,j},\ i\in\mathcal{I},\ 1\le n\le N,\\ V_{0,j}^{*}=(I-\mu\delta_y^2)U_{0,j}^{n},\quad V_{M_1,j}^{*}=(I-\mu\delta_y^2)U_{M_1,j}^{n},\quad 1\le n\le N.\end{cases} \tag{3.51}$$

After getting $V_{i,j}^{*}$, then we solve the following system to find the final numerical solution $U_{i,j}^{n}$, for fixed $i\in\{1,2,...,M_1-1\}$

$$\begin{cases}(I-\mu\delta_y^2)U_{i,j}^{n}=V_{i,j}^{*},\quad 1\le j\le M_2-1,\\ U_{i,0}^{n}=\Phi(x_i,y_0,t_n),\quad U_{i,M_2}^{n}=\Phi(x_i,y_{M_2},t_n).\end{cases} \tag{3.52}$$

3.4 Stability Analysis of the Schemes

Here, we discuss the stability bound of the nonuniform $L1$ difference scheme (3.50) for the nonlinear TFMDW equation (3.1) in detail.

Lemma 3.4.1. The solution U_i^n of the discrete difference scheme (3.45) satisfies the following bound

$$\|U^n\|_\infty \leq \|U^{n-1}\|_\infty + \left[\frac{\hat{c}_1}{\tau_n^\beta} + \frac{\hat{c}_2}{\tau_n^\alpha}\right]^{-1}\Bigg[\Lambda_{n-1}\|U^0\|_\infty + B_n\|\delta_t U^0\|_\infty + \|f^n\|_\infty + \mathrm{Im}_n\|U^{n-1}\|_\infty + \frac{Z(n)}{\tau_{n-1}}\|U^{n-2}\|_\infty + \sum_{k=1}^{n-2}(\Lambda_{n-k-1} - \Lambda_{n-k})\|U^k\|_\infty\Bigg], \tag{3.53}$$

where, $\mathrm{Im}_n = \frac{Z(n)}{\tau_{n-1}} + \Lambda_1 + \mathcal{L}$, and $\hat{c}_1$, $\hat{c}_2$ are positive constants.

Proof. The difference scheme defined in (3.45) can be rewrite as:

$$\left[\mathfrak{I}_n + \frac{2}{h^2}\right]U_i^n = \mathfrak{I}_n U_i^{n-1} + \frac{1}{h^2}(U_{i+1}^n + U_{i-1}^n) + \frac{Z(n)}{\tau_{n-1}}(U_i^{n-1} - U_i^{n-2}) - \Lambda_1 U_i^{n-1} + \Lambda_{n-1}U_i^0 + \sum_{k=1}^{n-2}(\Lambda_{n-k-1} - \Lambda_{n-k})U_i^k - \widetilde{F}(U_i^{n-1}) + f_i^n - B_n\delta_t U_i^0. \tag{3.54}$$

For fix $n \in \{1, 2, ..., N\}$, suppose i_o such that $\|U^n\|_\infty = \max\limits_{0\leq i\leq M}|U_i^n| = |U_{i_o}^n|$. Then equation (3.54) at mesh point (x_{i_o}, t_n) is

$$\left[\mathfrak{I}_n + \frac{2}{h^2}\right]U_{i_o}^n = \mathfrak{I}_n U_{i_o}^{n-1} + \frac{1}{h^2}(U_{i_o+1}^n + U_{i_o-1}^n) + \frac{Z(n)}{\tau_{n-1}}(U_{i_o}^{n-1} - U_{i_o}^{n-2}) - \Lambda_1 U_{i_o}^{n-1} + \Lambda_{n-1}U_{i_o}^0 + \sum_{k=1}^{n-2}(\Lambda_{n-k-1} - \Lambda_{n-k})U_{i_o}^k - \widetilde{F}(U_{i_o}^{n-1}) + f_{i_o}^n - B_n\delta_t U_{i_o}^0. \tag{3.55}$$

Using the inequality $|F(U)| \leq \mathcal{L}|U|$ and the selection of i_o, we obtain

$$\left[\mathfrak{I}_n + \frac{2}{h^2}\right]\|U^n\|_\infty \leq \mathfrak{I}_n\|U^{n-1}\|_\infty + \frac{2}{h^2}\|U^n\|_\infty + (\Lambda_1 + \mathcal{L})\|U^{n-1}\|_\infty + \Lambda_{n-1}\|U^0\|_\infty + B_n\|\delta_t U^0\|_\infty + \|f^n\|_\infty + \left|\frac{Z(n)}{\tau_{n-1}}(U_{i_o}^{n-1} - U_{i_o}^{n-2}) + \sum_{k=1}^{n-2}(\Lambda_{n-k-1} - \Lambda_{n-k})U_{i_o}^k\right|, \tag{3.56}$$

where, $\mathfrak{I}_n$ defined in equation (3.42). Now, using the values of A_1 and B_1 from equations (3.14) and (3.15), respectively in equation (3.42), we obtain

$$\begin{aligned} A_1 &= \frac{1}{\Gamma(2-\beta)} \frac{(t_n - t_{n-\frac{3}{2}})^{1-\beta} - (t_n - t_{n-\frac{1}{2}})^{1-\beta}}{\tau_{n-1}+\tau_n} \\ &= \frac{1}{\Gamma(2-\beta)} \frac{(2\tau_n + \tau_{n-1})^{1-\beta} - \tau_n^{1-\beta}}{2^{1-\beta}(\tau_{n-1}+\tau_n)}, \\ &= \frac{\tau_n^{-\beta}}{2^{1-\beta}\Gamma(2-\beta)} \frac{(2+\frac{\tau_{n-1}}{\tau_n})^{1-\beta} - 1}{1+\frac{\tau_{n-1}}{\tau_n}} := c_1\ W(n), \end{aligned} \tag{3.57}$$

where, $c_1 > 0$ for $0 < \beta < 1$, and

$$\begin{aligned} B_1 &= \frac{2}{\Gamma(3-\alpha)} \frac{(t_n - t_{n-\frac{3}{2}})^{2-\alpha} - (t_n - t_{n-\frac{1}{2}})^{2-\alpha}}{\tau_{n-1}+\tau_n} \\ &= \frac{2}{\Gamma(3-\alpha)} \frac{(2\tau_n + \tau_{n-1})^{2-\alpha} - \tau_n^{2-\alpha}}{2^{2-\alpha}(\tau_{n-1}+\tau_n)}, \\ &= \frac{2^{\alpha-1}}{\Gamma(3-\alpha)} \frac{\tau_n^{2-\alpha}}{\tau_{n-1}+\tau_n} \left[\left(2+\frac{\tau_{n-1}}{\tau_n}\right)^{2-\alpha} - 1 \right]; = c_2\ Z(n), \end{aligned} \tag{3.58}$$

where, $c_2 > 0$, for $1 < \alpha < 2$. Then

$$\mathfrak{I}_n := \frac{(1+c_1)}{\Gamma(2-\beta)} \frac{\tau_n^{-\beta}}{2^{1-\beta}} + \frac{(1+c_2)}{\Gamma(3-\alpha)} \frac{\tau_n^{-\alpha}}{2^{1-\alpha}} = \frac{\hat{c}_1}{\tau_n^{\beta}} + \frac{\hat{c}_2}{\tau_n^{\alpha}}, \tag{3.59}$$

where, $\hat{c}_1 > 0$ and $\hat{c}_2 > 0$. Then equation (3.56) equivalent to

$$\begin{aligned} \|U^n\|_\infty \le \|U^{n-1}\|_\infty + \left[\frac{\hat{c}_1}{\tau_n^{\beta}} + \frac{\hat{c}_2}{\tau_n^{\alpha}}\right]^{-1} \Bigg[\Lambda_{n-1}\|U^0\|_\infty + B_n\|\delta_t U^0\|_\infty + \|f^n\|_\infty \\ + (\Lambda_1 + \mathcal{L})\|U^{n-1}\|_\infty + \left| \frac{Z(n)}{\tau_{n-1}}(U_{i_o}^{n-1} - U_{i_o}^{n-2}) + \sum_{k=1}^{n-2} (\Lambda_{n-k-1} - \Lambda_{n-k}) U_{i_o}^{k} \right| \Bigg]. \end{aligned} \tag{3.60}$$

Thus we get the desired result easily. □

Now, we analyze the stability of the difference scheme (3.50). Suppose $U_{i,j}^n$ and $u_{i,j}^n$ are the numerical and exact solutions of the considered problem (3.1)-(1.14). Let

$$\Theta_{i,j}^n = U_{i,j}^n - u_{i,j}^n, \quad (i,j) \in \mathcal{I}, \quad 1 \leq n \leq N. \tag{3.61}$$

We obtain the following roundoff error equation of the difference scheme (3.50) by using (3.61)

$$\begin{aligned}(I-\mu\delta_x^2)(I-\mu\delta_y^2)\Theta_{i,j}^n &= \left[1+\mu\frac{Z(n)}{\tau_{n-1}}\right]\left(\Theta_{i,j}^{n-1}+\mu^2\delta_x^2\delta_y^2\Theta_{i,j}^{n-1}\right)-\mu\frac{Z(n)}{\tau_{n-1}}\left(\Theta_{i,j}^{n-2}\right.\\ &\left.+\mu^2\delta_x^2\delta_y^2\Theta_{i,j}^{n-2}\right)+\mu\sum_{k=1}^{n-2}\left[(\Lambda_{n-k-1}-\Lambda_{n-k})\left(\Theta_{i,j}^k+\mu^2\delta_x^2\delta_y^2\Theta_{i,j}^k\right)\right.\\ &\left.+\Lambda_{n-1}\left(\Theta_{i,j}^0+\mu^2\delta_x^2\delta_y^2\Theta_{i,j}^0\right)\right]-\mu\Lambda_1\left(\Theta_{i,j}^{n-1}+\mu^2\delta_x^2\delta_y^2\Theta_{i,j}^{n-1}\right)\\ &-\mu[\widetilde{F}(U_{i,j}^{n-1})-\widetilde{F}(u_{i,j}^{n-1})]+\mu B_n\delta_t\Theta_{i,j}^0, \quad 1\leq n\leq N.\end{aligned} \tag{3.62}$$

Using the inequality $|F(U_{i,j}^{n-1})-F(u_{i,j}^{n-1})| \leq \mathcal{L}|U_{i,j}^{n-1}-u_{i,j}^{n-1}|$ from Lipschitz condition.

$$\begin{aligned}(I-\mu\delta_x^2)(I-\mu\delta_y^2)\Theta_{i,j}^n &= \left[1+\mu\frac{Z(n)}{\tau_{n-1}}\right]\left(\Theta_{i,j}^{n-1}+\mu^2\delta_x^2\delta_y^2\Theta_{i,j}^{n-1}\right)-\mu\frac{Z(n)}{\tau_{n-1}}\left(\Theta_{i,j}^{n-2}\right.\\ &\left.+\mu^2\delta_x^2\delta_y^2\Theta_{i,j}^{n-2}\right)+\mu\sum_{k=1}^{n-2}\left[(\Lambda_{n-k-1}-\Lambda_{n-k})\left(\Theta_{i,j}^k+\mu^2\delta_x^2\delta_y^2\Theta_{i,j}^k\right)+\Lambda_{n-1}\Theta_{i,j}^0\right]\\ &-\mu\Lambda_1\left(\Theta_{i,j}^{n-1}+\mu^2\delta_x^2\delta_y^2\Theta_{i,j}^{n-1}\right)-\mu\mathcal{L}\Theta_{i,j}^{n-1}+\mu B_n\delta_t\Theta_{i,j}^0, \quad (i,j)\in\mathcal{I}, \quad 1\leq n\leq N.\end{aligned} \tag{3.63}$$

Now, we construct the grid function $\Theta(x,y)$ as follows , for $n=1,2,...,N$

$$\Theta^n(x,y)=\begin{cases}\Theta^n_{i,j}\ , & x_{i-\frac{1}{2}}<x\leq x_{i+\frac{1}{2}},\ y_{j-\frac{1}{2}}<y\leq y_{j+\frac{1}{2}}\\ & 1\leq i\leq M_1-1,\quad 1\leq j\leq M_2-1,\\ 0\ \ , & 0\leq x\leq \frac{h_1}{2},\quad L_1-\frac{h_1}{2}<x\leq L_1,\\ & 0\leq y\leq \frac{h_2}{2},\quad L_2-\frac{h_2}{2}<y\leq L_2.\end{cases}\tag{3.64}$$

The expression of the function $\Theta^n(x,y)$ in Fourier series form is given as

$$\Theta^n(x,y)=\sum_{n_1=-\infty}^{\infty}\sum_{n_2=-\infty}^{\infty}\xi^n(n_1,n_2)e^{2\pi\iota(n_1x/L_1+n_2y/L_2)},\qquad n\geq 1,\tag{3.65}$$

where

$$\xi^n(n_1,n_2)=\frac{1}{L_1\ L_2}\int_0^{L_1}\int_0^{L_2}\Theta^n(x,y)e^{-2\pi\iota(n_1x/L_1+n_2y/L_2)}dxdy.\tag{3.66}$$

Suppose the solution of equation (3.62) is $\Theta^n_{i,j}=\xi^n e^{\iota(i\epsilon_1h_1+j\epsilon_2h_2)}$, where $\epsilon_1=2\pi n_1/L_1$, $\epsilon_2=2\pi n_2/L_2$, and $\iota=\sqrt{-1}$. It can be easily obtained as

$$\delta_x^2\Theta^n_{i,j}:=\frac{1}{h_1^2}(\Theta^n_{i+1,j}-2\Theta^n_{i,j}+\Theta^n_{i-1,j})=-\frac{4}{h_1^2}\sin^2\left(\frac{\epsilon_1h_1}{2}\right)\xi^n e^{\iota(i\epsilon_1h_1+j\epsilon_2h_2)},\tag{3.67}$$

similarly,

$$\delta_y^2\Theta^n_{i,j}=-\frac{4}{h_2^2}\sin^2\left(\frac{\epsilon_2h_2}{2}\right)\xi^n e^{\iota(i\epsilon_1h_1+j\epsilon_2h_2)},\tag{3.68}$$

$$\delta_x^2\delta_y^2\Theta^n_{i,j}=\frac{16}{h_1^2h_2^2}\sin^2\left(\frac{\epsilon_1h_1}{2}\right)\sin^2\left(\frac{\epsilon_2h_2}{2}\right)\xi^n e^{\iota(i\epsilon_1h_1+j\epsilon_2h_2)}.\tag{3.69}$$

Using the defined solution $\Theta_{i,j}^{n}$ and expressions (3.67)-(3.69) into equation (3.63), we get

$$\begin{aligned}\left[1+\frac{4\mu}{h_1^2}\sin^2\left(\frac{\epsilon_1 h_1}{2}\right)\right]\left[1+\frac{4\mu}{h_2^2}\sin^2\left(\frac{\epsilon_2 h_2}{2}\right)\right]\xi^n &= \left[1+\mu\frac{Z(n)}{\tau_{n-1}}-\mu\Lambda_1\right]\\ \left[1+\frac{16\mu^2}{h_1^2h_2^2}\sin^2\left(\frac{\epsilon_1 h_1}{2}\right)\sin^2\left(\frac{\epsilon_2 h_2}{2}\right)\right]\xi^{n-1}-\mu\frac{Z(n)}{\tau_{n-1}}&\left[1+\frac{16\mu^2}{h_1^2h_2^2}\sin^2\left(\frac{\epsilon_1 h_1}{2}\right)\right.\\ \left.\sin^2\left(\frac{\epsilon_2 h_2}{2}\right)\right]\xi^{n-2}+\mu&\left[1+\frac{16\mu^2}{h_1^2h_2^2}\sin^2\left(\frac{\epsilon_1 h_1}{2}\right)\sin^2\left(\frac{\epsilon_2 h_2}{2}\right)\right]\\ \sum_{k=1}^{n-2}\left[\left(\Lambda_{n-k-1}-\Lambda_{n-k}\right)\xi^k+\Lambda_{n-1}\xi^0\right]&-\mu\mathcal{L}\xi^{n-1}. \end{aligned}\tag{3.70}$$

Let,

$$H_1=\frac{4\mu}{h_1^2}\sin^2\left(\frac{\epsilon_1 h_1}{2}\right)\geq 0,\qquad H_2=\frac{4\mu}{h_1^2}\sin^2\left(\frac{\epsilon_1 h_1}{2}\right)\geq 0.$$

Then, equation (3.70) yields

$$\begin{aligned}(1+H_1)(1+H_2)\xi^n=(1+H_1H_2)\Bigg\{&\left[1-\mu\Lambda_1-\mu\mathcal{L}\right]\xi^{n-1}+\left[\mu\frac{Z(n)}{\tau_{n-1}}\right]\\ &\left(\xi^{n-1}-\xi^{n-2}\right)+\mu\sum_{k=1}^{n-2}\left[\left(\Lambda_{n-k-1}-\Lambda_{n-k}\right)\xi^k+\Lambda_{n-1}\xi^0\right]\Bigg\}.\end{aligned}\tag{3.71}$$

Using the hypothesis $\tau_{n-1}\leq\tau_n,\ \ 2\leq n\leq N$. Then we get following inequality

$$\xi^n\leq(1+H_1H_2)\left[\frac{\xi^{n-1}+\mu\frac{Z(n)}{\tau_{n-1}}(\xi^{n-1}-\xi^{n-2})+\mu\sum_{k=1}^{n-2}\left[\left(\Lambda_{n-k-1}-\Lambda_{n-k}\right)\xi^k+\Lambda_{n-1}\xi^0\right]}{(1+H_1)(1+H_2)}\right].\tag{3.72}$$

Lemma 3.4.2. For small value of h_1 and h_2, the following inequality holds:

$$\frac{\left|\left[1+\frac{16\mu_n^2}{h_1^2h_2^2}\sin^2\left(\frac{\epsilon_1 h_1}{2}\right)\sin^2\left(\frac{\epsilon_2 h_2}{2}\right)\right]\right|}{\left|\left[1+\frac{4\mu_n}{h_1^2}\sin^2\left(\frac{\epsilon_1 h_1}{2}\right)\right]\left[1+\frac{4\mu_n}{h_1^2}\sin^2\left(\frac{\epsilon_2 h_2}{2}\right)\right]\right|}\leq 1,\qquad\forall n\geq 1.\tag{3.73}$$

Lemma 3.4.3. Suppose that ξ^n, $1 \leq n \leq N$ are the solutions of equation (3.72), then

$$|\xi^n| \leq |\xi^0|, \quad 1 \leq n \leq N. \tag{3.74}$$

Proof. We use induction argument and Lemma 3.4.2 to prove bound for $|\xi^n|$ in terms of $|\xi^0|$. For $n = 1$,

$$|\xi^1| \leq \left| \frac{(1 + H_1 H_2)}{(1 + H_1)(1 + H_2)} \xi^0 \right| \leq |\xi^0|. \tag{3.75}$$

Now suppose that

$$|\xi^n| \leq |\xi^0|, \quad n = 1, 2, ..., r - 1. \tag{3.76}$$

By setting $n = r$ in equation (3.72) and then using the equation (3.39) and (3.76), we obtain

$$|\xi^r| \leq \frac{\left| \left[1 + \frac{16\mu_n^2}{h_1^2 h_2^2} \sin^2\left(\frac{\epsilon_1 h_1}{2}\right) \sin^2\left(\frac{\epsilon_2 h_2}{2}\right) \right] \right|}{\left| \left[1 + \frac{4\mu_n}{h_1^2} \sin^2\left(\frac{\epsilon_1 h_1}{2}\right) \right] \left[1 + \frac{4\mu_n}{h_1^2} \sin^2\left(\frac{\epsilon_2 h_2}{2}\right) \right] \right|} |\xi^0|. \tag{3.77}$$

Using the Lemma 3.4.2 in above result (3.77), we get desired result. □

3.5 Numerical Results

In this section, we carry five numerical examples corresponding to model (3.1) to verify theoretical accuracy of the numerical schemes defined in (3.45) and (3.51)-(3.52) for solving the 1D and 2D nonlinear TFMDW equation respectively. We use nonuniform meshes to achieve the theoretical OC if there is a strong singularity in the exact solution of nonlinear TFMDW equation at $t = 0$. To validate the discussed

difference schemes (3.45) and (3.51)-(3.52), we select $F(u)$ as:

$$\textbf{Case 1}\ \ F(u) = u^3 - 2u, \quad \textbf{Case 2}\ \ F(u) = \sin(u), \quad \textbf{Case 3}\ \ F(u) = u^2.$$

We use the following formulas to estimate the error and rate of convergence in 1D nonlinear TFMDW equation

$$E_1(h,\tau) = \max_{1\le i\le M-1} ||U(x_i,t_N) - u(x_i,t_N)||_\infty,$$
$$r_t = log_2\left[\frac{E_1(h,2\tau)}{E_1(h,\tau)}\right], \quad r_s = log_2\left[\frac{E_1(2h,\tau)}{E_1(h,\tau)}\right],$$

where $U(x_i,t_N)$ and $u(x_i,t_N)$ denote the approximate and exact solutions of the problem (3.1) in one dimension.

Example 3.5.1. Consider 1D Klein-Gordon TFMDW equation (3.1) with domain $(x,t) \in [0,1]\times[0,1]$

$${}^C\mathcal{D}^{\beta}_{0,t}u(x,t) + {}^C\mathcal{D}^{\alpha}_{0,t}u(x,t) + F(u(x,t)) = \frac{\partial^2 u(x,t)}{\partial x^2} + f(x,t).$$

The zero initial and boundary conditions with source term $f(x,t) = \left(\frac{\Gamma(\delta+1)}{\Gamma(\delta+1-\beta)}t^{\delta-\beta} + \frac{\Gamma(\delta+1)}{\Gamma(\delta+1-\alpha)}t^{\delta-\alpha} + \pi^2 t^{\delta}\right)\sin(\pi x) + F(u(x,t))$ are chosen from the exact solution $u(x,t) = t^{\delta}\sin(\pi x)$, and nonlinear term is $F(u(x,t)) = u^3 - 2u$.

In Tables 3.1-3.4, we give the maximum absolute error and convergence order of the proposed scheme (3.45) in the temporal direction. Tables 3.1-3.3, show the error and OC for uniform mesh ($\gamma = 1$) as exact solution is sufficiently smooth, and Table 3.4 represents the numerical results with nonuniform meshes. Tables 3.1-3.3 display the numerical results for different sets of values of fractional parameters (β,α) with space step length $h = \frac{1}{500}$. In Table 3.4, we observe that the scheme achieves OC $\min(2-\beta, 3-\alpha, \gamma\beta, \gamma(\alpha-1))$ for $\gamma = 2,\ 3$ with different values of the

parameters β, α and $M = 200$. Tables 3.1-3.4, express that the proposed scheme is efficiently accurate and the numerical results have agreement with the theoretical OC $\min(2-\beta, 3-\alpha, \gamma\beta, \gamma(\alpha-1))$.

TABLE 3.1: Maximum absolute errors and OC in time direction for Example 3.5.1 with $\delta = 3$, $M = 500$ and varying values of β, α.

	$\beta = 0.2, \alpha = 1.8$		$\beta = 0.3, \alpha = 1.6$		$\beta = 0.7, \alpha = 1.3$		
τ	$\|u^\tau - U^\tau\|_\infty$	OC	$\|u^\tau - U^\tau\|_\infty$	OC	$\|u^\tau - U^\tau\|_\infty$	OC	CPU(s)
$1/2^5$	1.1985E-02		5.1121E-03		4.0216E-03		1.187264
$1/2^6$	5.0479E-03	1.2474	1.8094E-03	1.4984	1.4442E-03	1.4775	1.719751
$1/2^7$	2.1360E-03	1.2408	6.4248E-04	1.4938	5.1487E-04	1.4880	2.879440
$1/2^8$	9.1239E-04	1.2272	2.3153E-04	1.4725	1.8722E-04	1.4595	4.973156
$1/2^9$	3.9308E-04	1.2148	8.5208E-05	1.4421	7.0400e-05	1.4111	9.710824

TABLE 3.2: Maximum absolute errors and OC in time direction for Example 3.5.1 with $\delta = 3$, $M = 500$ and varying values of β, α.

	$\beta = 0.5, \alpha = 1.6$		$\beta = 0.7, \alpha = 1.6$		$\beta = 0.95, \alpha = 1.6$		
τ	$\|u^\tau - U^\tau\|_\infty$	OC	$\|u^\tau - U^\tau\|_\infty$	OC	$\|u^\tau - U^\tau\|_\infty$	OC	CPU(s)
$1/2^5$	5.6145E-03		6.8085E-03		1.0669E-02		1.286321
$1/2^6$	2.0196E-03	1.4751	2.5714E-03	1.4048	4.6355E-03	1.2027	1.843045
$1/2^7$	7.2568E-04	1.4766	9.7023E-04	1.4061	2.0388E-03	1.1850	2.855537
$1/2^8$	2.6345E-04	1.4618	3.6924E-04	1.3938	9.1218E-04	1.1603	4.950344
$1/2^9$	9.7214E-05	1.4383	1.4228E-04	1.3758	4.1485E-04	1.1367	10.68066

In Figure 3.1, we display the absolute error graphs for different choices of fractional parameters (β, α) by using scheme (3.45) for 1D nonlinear TFMDW equation. Figures 3.1**(a)** and 3.1**(b)** represent the absolute errors for $\beta = 0.2$, $\alpha = 1.2$ and $\beta = 0.8$, $\alpha = 1.8$, respectively with the smooth case of the solution i.e. $\delta = 3$. In Figure 3.3, we compare the absolute error for Example 3.5.1 on nonuniform and uniform grids

for $\beta = 0.5$, $\alpha = 1.25$ and $M = N = 50$. We see that the error is decreasing for higher values of γ as compare to $\gamma = 1$ which indicates that the proposed scheme (3.45) works well with nonuniform meshes. From Figure 3.2, we observe that the slope of the approximate solutions follow similar pattern as of line $y = 2x$ which confirms that the proposed scheme has twice spatial order of convergence.

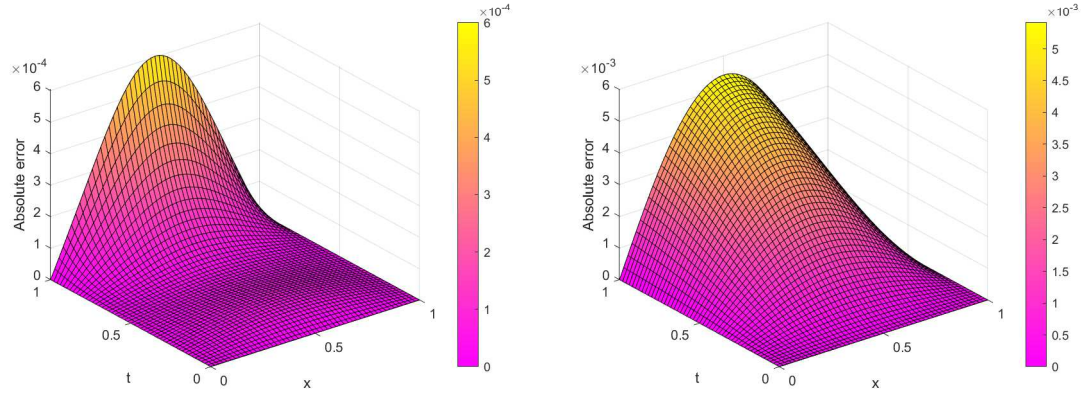

(a) Scheme (3.45) with $\beta = 0.2$, $\alpha = 1.2$.

(b) Scheme (3.45) with $\beta = 0.8$, $\alpha = 1.8$.

FIGURE 3.1: Absolute error surfaces for Example 3.5.1 with $\delta = 3$, $\gamma = 1$ and $M = N = 50$.

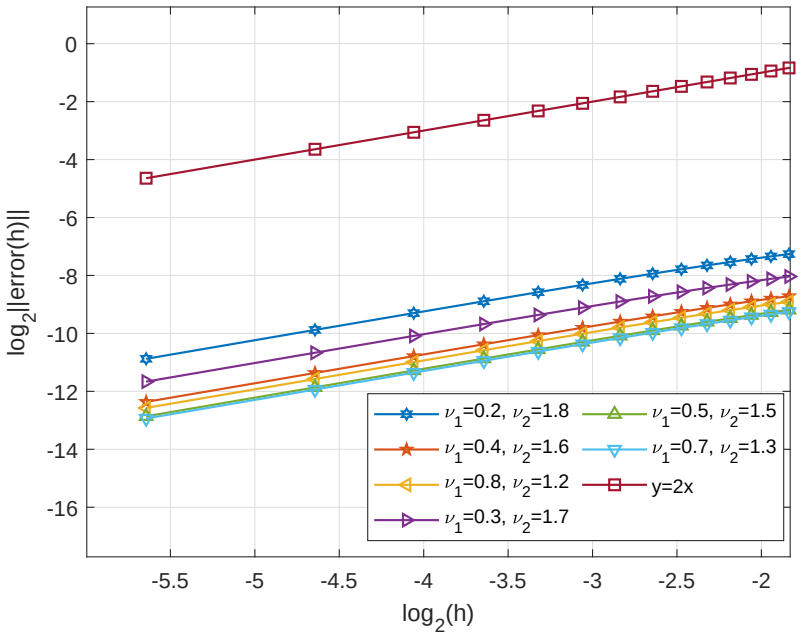

FIGURE 3.2: The rate of convergence in space direction for Example 3.5.1 with different values of pairs (β, α), $\delta = 3$ and $M = N = 50$.

TABLE 3.3: Maximum absolute errors and OC in time direction for Example 3.5.1 with $\delta = 3$, $M = 500$ and varying values of β, α.

	$\beta = 0.3, \alpha = 1.3$		$\beta = 0.5, \alpha = 1.5$		$\beta = 0.8, \alpha = 1.8$		
τ	$\|u^\tau - U^\tau\|_\infty$	OC	$\|u^\tau - U^\tau\|_\infty$	OC	$\|u^\tau - U^\tau\|_\infty$	OC	CPU(s)
$1/2^5$	2.5106E-03		4.1917E-03		1.4526E-02		1.221002
$1/2^6$	7.8304E-04	1.6809	1.4332E-03	1.5484	6.2861E-03	1.2083	1.749084
$1/2^7$	2.3154E-04	1.7579	4.8363E-04	1.5672	2.7102E-03	1.2138	2.777732
$1/2^8$	6.7759E-05	1.7728	1.6420E-04	1.5585	1.1713E-03	1.2103	4.821588
$1/2^9$	2.0650E-05	1.7142	5.6920E-05	1.5284	5.0799E-04	1.2052	9.247415

Figure 3.4 displays the behavior of the uniform and nonuniform meshes near singularity at $t = 0$ for Example 3.5.1. In graphs 3.4**(a)** and 3.4**(b)**, we represent the absolute error with $(\beta, \alpha) = (0.5, 1.5)$, $T = 1$, $M = N = 50$ for the case of non smooth solution i.e. $\delta = \alpha$ in Example 3.5.1. From Figure 3.4**(a)**, we can see that

the error blows-up near the singularity $t = 0$ and after that it decreases smoothly. To handle such behavior of error, we take nonuniform mesh by selecting $\gamma = 2$ and display the absolute error in the Figure 3.4**(b)**. In Table 3.5, we compare our described scheme (3.45) and the scheme used in [2] with $M = 500$, $\beta = 0.5$, $\alpha = 1.5$ at the final time $T = 1$. One can observe that the discussed method is in agreement with the theoretical findings in less computational time as compared to the CPU (in seconds) time of the scheme given in [2].

TABLE 3.4: Maximum absolute errors and OC in time direction for Example 3.5.1 with $\delta = \alpha$, $M = 200$ and varying values of β, α, γ.

	$\gamma = 1$		$\gamma = 2$		$\gamma = 3$		$\beta = 0.8$
	$\beta = 0.5, \alpha = 1.5$		$\beta = 0.5, \alpha = 1.5$		$\beta = 0.8, \alpha = 1.4$		$\alpha = 1.4$
τ	$\|u^\tau - U^\tau\|_\infty$	OC	$\|u^\tau - U^\tau\|_\infty$	OC	$\|u^\tau - U^\tau\|_\infty$	OC	CPU(s)
1/160	2.0054E-03		1.5357E-03		1.9277E-03		1.209560
1/320	1.9560E-03	0.03596	7.5862E-04	1.0174	9.7332E-04	0.9859	1.699615
1/640	1.6805E-03	0.21903	3.7221E-04	1.0273	4.8876E-04	0.9938	3.097869
1/1280	1.3470E-03	0.31916	1.7992E-04	1.0488	2.4272E-04	1.0098	8.395788
1/2560	1.0354E-03	0.37946	8.4187E-05	1.0957	1.1788E-04	1.0420	45.40611
1/5120	7.7512E-04	0.41776	3.6600E-05	1.2017	5.4679E-05	1.1083	245.4984
1/10240	5.7025E-04	0.44282	1.3181E-05	1.4734	2.2922E-05	1.2542	1409.409

TABLE 3.5: Maximum absolute errors and OC in time direction for Example 1 of [2] with $M = 500$.

	Scheme (3.45)		[2]		Scheme (3.45)	[2]
	$\beta = 0.5, \alpha = 1.5$		$\beta = 0.5, \alpha = 1.5$			
τ	$\|u^\tau - U^\tau\|_\infty$	OC	$\|u^\tau - U^\tau\|_\infty$	OC	CPU	CPU
5	6.4560E-02		3.9393E-02		0.929317	0.55
10	2.5320E-02	1.3504	1.5505E-02	1.34	1.099860	1.29
20	8.9756E-03	1.4962	5.4021E-03	1.52	1.326152	2.12
40	3.0763E-03	1.5448	1.8141E-03	1.57	1.642594	3.50
80	1.0459E-03	1.5565	6.1968E-04	1.54	2.271350	6.08
160	3.5715E-04	1.5501	*	*	3.427004	*
320	1.2353E-04	1.5317	*	*	5.982780	*
640	4.3792E-05	1.4961	*	*	12.39335	*

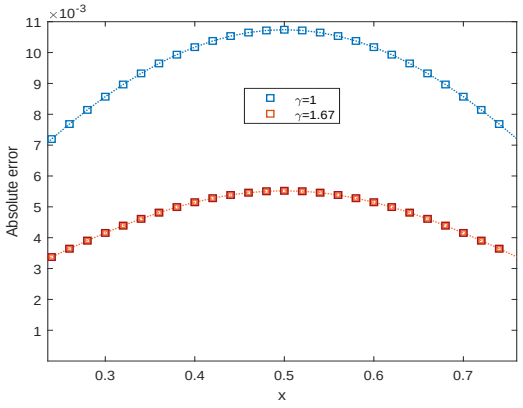

FIGURE 3.3: Comparison of absolute error between uniform ($\gamma = 1$) and nonuniform ($\gamma = 1.67$) mesh for Example 3.5.1 with $\beta = 0.5$, $\alpha = 1.25$, $\delta = \alpha$ and $M = N = 50$.

In Table 3.6, we display the error on L_∞ norm and OC of the analyzed difference scheme (3.45) in space direction by taking fixed time step length as $\tau = \frac{1}{5000}$. The presented results are carried out for different pairs of values of (δ, γ) and (β, α). From the Table 3.6, one can note that the spatial convergence accuracy is of second-order.

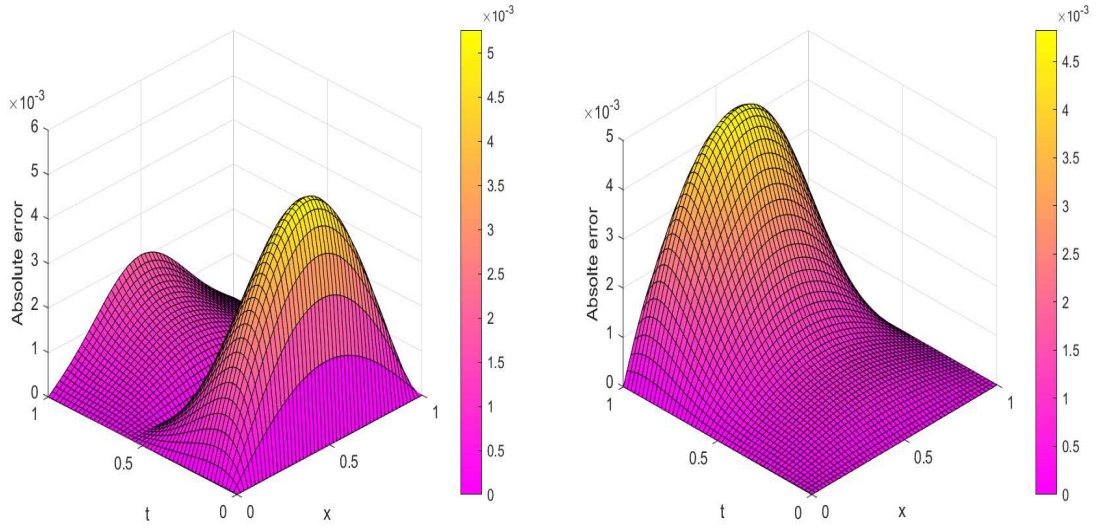

(a) Scheme with $\gamma = 1$ and $\beta = 0.5$, $\alpha = 1.5$.

(b) Scheme with $\gamma = 2$ and $\beta = 0.5$, $\alpha = 1.5$.

FIGURE 3.4: Absolute error graphs for Example 3.5.1 on the uniform **(a)** and nonuniform **(b)** meshes with $M = N = 50$, $\delta = \alpha$.

TABLE 3.6: Maximum absolute errors and OC in space direction for Example 3.5.1 with $\tau = \frac{1}{5000}$ and varying values of β, α.

		$\beta = 0.3, \alpha = 1.7$		$\beta = 0.5, \alpha = 1.5$		$\beta = 0.7, \alpha = 1.3$	
M	(δ, γ)	$\|u^\tau - U^\tau\|_\infty$	OC	$\|u^\tau - U^\tau\|_\infty$	OC	$\|u^\tau - U^\tau\|_\infty$	OC
4	$(3, 1)$	2.6551E-02		2.9386E-02		3.0817E-02	
8		6.6625E-03	1.9946	7.3442E-03	2.0004	7.6910E-03	2.0025
16		1.6752E-03	1.9917	1.8371E-03	1.9991	1.9241E-03	1.9990
	CPU	69.553496		139.415052		206.774764	
4	$(\alpha, 2.5)$	3.8941E-02		4.0582E-02		4.1006E-02	
8		9.7099E-03	2.0038	1.0087E-02	2.0083	1.0244E-02	2.0011
16		2.4242E-03	2.0020	2.5185E-03	2.0019	2.6158E-03	1.9694
	CPU	73.374518		141.858775		232.028216	

Example 3.5.2. We consider the 2D nonlinear TFMDW equation (3.1) with $L_1 = L_2 = \pi$ and $T = 1$

$$ {}^{C}\mathcal{D}^{\beta}_{0,t}u(x,y,t) + {}^{C}\mathcal{D}^{\alpha}_{0,t}u(x,y,t) + F(u(x,y,t)) = \Delta u(x,y,t) + f(x,y,t). $$

Suppose the exact solution of the problem is $u(x,y,t) = t^4 \sin(x)\sin(y)$ then the corresponding initial and boundary conditions are zero and source term is

$$ f(x,y,t) = \left[\frac{24}{\Gamma(5-\beta)}t^{4-\beta} + \frac{24}{\Gamma(5-\alpha)}t^{4-\alpha} + 2t^4\right]\sin(x)\sin(y) + F(u(x,y,t)). $$

Let $h_1 = h_2 = h$ be the spatial step-sizes. To compute the error in 2D nonlinear TFMDW problem, we use the following formula

$$ E_2(h,\tau) = \max_{\substack{1\le i\le M_1-1\\ 1\le j\le M_2-1}} ||U(x_i,y_j,t_N) - u(x_i,y_j,t_N)||_\infty, $$

where $U(x_i,y_j,t_N)$ and $u(x_i,y_j,t_N)$ denote the approximate and exact solutions of the problem (3.1) at the final time $T = 1$. We use the following formulas to find the OC in temporal and spatial direction for the proposed ADI scheme (3.51)-(3.52) corresponding to the maximum norm.

$$ r_t = log_2\left[\frac{E_2(h,2\tau)}{E_2(h,\tau)}\right], \quad r_s = log_2\left[\frac{E_2(2h,\tau)}{E_2(h,\tau)}\right]. $$

Tables 3.7, 3.8, 3.9, display the maximum absolute errors and convergence accuracies of the ADI scheme (3.51)-(3.52) in time direction for Example 3.5.2. In Example 3.5.2, we deal with all three cases of $F(u)$ to investigate numerical schemes (3.45) and (3.51)-(3.52) in the considered domain $[0,\pi]^2 \times [0,1]$. Tables 3.7, 3.8, 3.9, represent the numerical experiments for $F(u) = \sin(u)$, $u^3 - 2u$, u^2, respectively with 50×50 uniform points and different choices of fractional parameters β, α. From the Tables,

one can note that the temporal OC is $\min(2-\beta, 3-\alpha)$ on the uniform meshes and numerical results are in agreement with this accuracy. In Figure 3.5, we express the surface of maximum absolute error at final time $T = 1$ with $M_1 = M_2 = 50$, $\tau = 0.002$ and $(\beta, \alpha) = (0.3, 1.5)$ for Example 3.5.2.

TABLE 3.7: Maximum absolute errors and OC in time direction for Example 3.5.2 with $F(u) = \sin(u)$, varying values of β, α and $h_1 = h_2 = \frac{\pi}{50}$.

	$\beta = 0.2, \alpha = 1.8$		$\beta = 0.4, \alpha = 1.7$		$\beta = 0.8, \alpha = 1.25$		
τ	$\|u^\tau - U^\tau\|_\infty$	OC	$\|u^\tau - U^\tau\|_\infty$	OC	$\|u^\tau - U^\tau\|_\infty$	OC	CPU(s)
$1/2^3$	1.2239E-01		9.2435E-02		5.9529E-02		0.353195
$1/2^4$	5.2297E-02	1.2267	3.6758E-02	1.3304	2.3754E-02	1.3254	0.978580
$1/2^5$	2.2510E-02	1.2162	1.4680E-02	1.3242	9.9971E-03	1.2486	2.807489
$1/2^6$	9.7411E-03	1.2084	5.8943E-03	1.3165	4.0784E-03	1.2935	9.290004
$1/2^7$	4.2362E-03	1.2013	2.3849E-03	1.3054	1.7497E-03	1.2209	33.64847

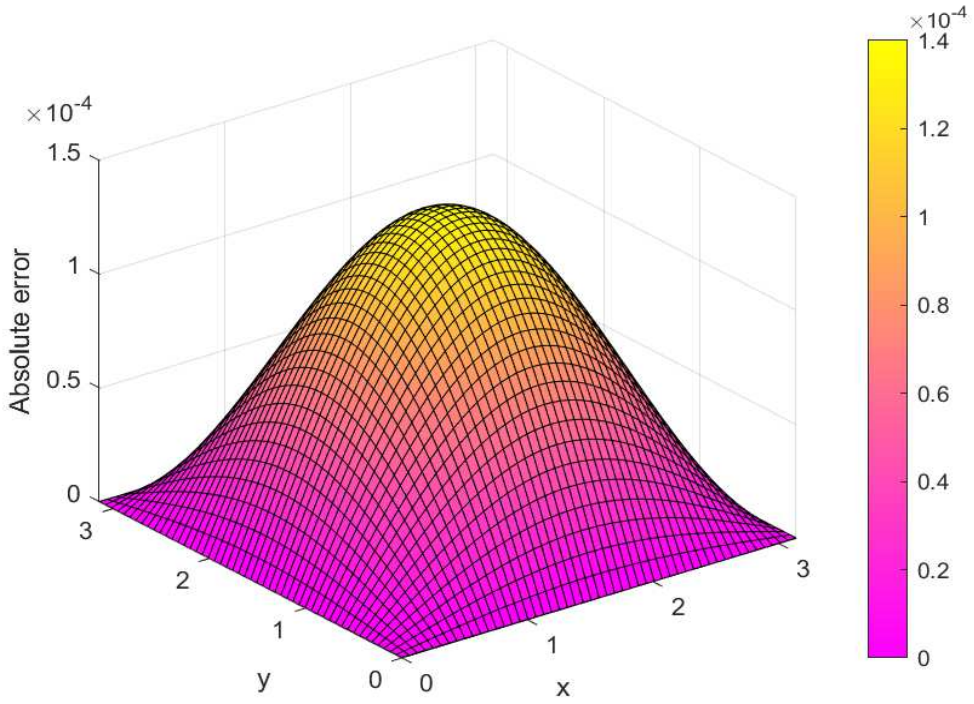

FIGURE 3.5: Absolute error graphs for Example 3.5.2 with $M = 50$, $N = 500$, $\beta = 0.3$, $\alpha = 1.5$ and $F(u) = u^3 - 2u$.

TABLE 3.8: Maximum absolute errors and OC in time direction for Example 3.5.2 with $F(u) = u^3 - 2u$, varying values of β, α and $h_1 = h_2 = \frac{\pi}{50}$.

	$\beta = 0.2, \alpha = 1.8$		$\beta = 0.4, \alpha = 1.7$		$\beta = 0.8, \alpha = 1.25$		
τ	$\|u^\tau - U^\tau\|_\infty$	OC	$\|u^\tau - U^\tau\|_\infty$	OC	$\|u^\tau - U^\tau\|_\infty$	OC	CPU(s)
$1/2^3$	1.3527E-01		1.0067E-01		6.4124E-02		0.242581
$1/2^4$	5.9700E-02	1.1800	4.1879E-02	1.2653	2.7796E-02	1.2060	0.836927
$1/2^5$	2.6241E-02	1.1859	1.7234E-02	1.2809	1.1888E-02	1.2254	2.679007
$1/2^6$	1.1505E-02	1.1896	7.0538E-03	1.2888	4.9726E-03	1.2574	9.125027
$1/2^7$	5.0411E-03	1.1904	2.8870E-03	1.2888	2.1371E-03	1.2183	33.25655

TABLE 3.9: Maximum absolute errors and OC in time direction for Example 3.5.2 with $F(u) = u^2$, varying values of β, α and $h_1 = h_2 = \frac{\pi}{50}$.

	$\beta = 0.3, \alpha = 1.3$		$\beta = 0.5, \alpha = 1.5$		$\beta = 0.8, \alpha = 1.8$		
τ	$\|u^\tau - U^\tau\|_\infty$	OC	$\|u^\tau - U^\tau\|_\infty$	OC	$\|u^\tau - U^\tau\|_\infty$	OC	CPU(s)
$1/2^3$	4.4042E-02		6.6310E-02		1.4413E-01		0.253837
$1/2^4$	1.4027E-02	1.6507	2.3180E-02	1.5163	6.1282E-02	1.2339	0.822873
$1/2^5$	4.2918E-03	1.7086	8.0213E-03	1.5310	2.6370E-02	1.2165	2.578670
$1/2^6$	1.2976E-03	1.7257	2.7870E-03	1.5251	1.1422E-02	1.2072	7.927668
$1/2^7$	4.1677E-04	1.6386	9.8845E-04	1.4955	4.9692E-03	1.2007	27.24583

In Table 3.10, we give the maximum error on L_∞ norm and convergence accuracy in space direction for Example 3.5.2 with $N = 10,000$. Table 3.10 shows the numerical results for $F(u) = u^3 - 2u$ with $\gamma = 1$ and different pairs of parameters (β, α). The Table 3.10 confirms that the ADI scheme (3.51)-(3.52) is second-order accurate in space.

TABLE 3.10: Maximum absolute errors and OC in space direction for Example 3.5.2 with $F(u) = u^3 - 2u$, varying values of β, α and $\tau = \frac{1}{10000}$.

	$\beta = 0.3, \alpha = 1.5$		$\beta = 0.5, \alpha = 1.3$		$\beta = 0.7, \alpha = 1.6$		
M	$\|u^\tau - U^\tau\|_\infty$	OC	$\|u^\tau - U^\tau\|_\infty$	OC	$\|u^\tau - U^\tau\|_\infty$	OC	CPU
4	7.2600E-03		9.0010E-03		5.7216E-03		1214.8286
8	1.8386E-03	1.9813	2.2782E-03	1.9822	1.4535E-03	1.9769	4780.3552
16	4.6208E-04	1.9924	5.7172E-04	1.9945	3.6905E-04	1.9776	18765.016

Example 3.5.3. In this example, we consider 1D nonlinear TFMDW equation on $(x,t) \in \Omega \times [0,1]$

$$
\begin{aligned}
&{}^C\mathcal{D}^{\beta}_{0,t}u(x,t) + {}^C\mathcal{D}^{\alpha}_{0,t}u(x,t) + u^3(x,t) - 2u(x,t) = \frac{\partial^2 u(x,t)}{\partial x^2} + f(x,t),\\
&u(x,0) = 0, \quad \frac{\partial u(x,0)}{\partial t} = 0, \quad x \in \Omega,\\
&u(0,t) = 0, \quad u(1,t) = (t^{\beta+1} + t^{\alpha})\sin(1), \quad (x,t) \in \partial\Omega \times (0,T].
\end{aligned}
$$

The nonsmooth exact solution of the equation (3.1) is given as $u(x,t) = (t^{\beta+1} + t^{\alpha})\sin(x)$, $(x,t) \in \Omega \times [0,1]$ and corresponding source term is

$$
\begin{aligned}
f(x,t) = \Bigg[&\frac{\Gamma(\beta+2)}{\Gamma(2)}\, t + \frac{\Gamma(\alpha+1)}{\Gamma(\alpha+1-\beta)}\, t^{\alpha-\beta} + \frac{\Gamma(\beta+2)}{\Gamma(\beta+2-\alpha)}\, t^{\beta+1-\alpha}\\
&+ \Gamma(\alpha+1) + t^{\beta+1} + t^{\alpha}\Bigg]\sin(x) + u^3(x,t) - 2u(x,t).
\end{aligned}
$$

We calculate this problem using scheme (3.45) in domain $(x,t) \in [0,1] \times [0,1]$. In Tables 3.11, 3.12, 3.13, we present maximum absolute errors and convergence rates in the time direction on nonuniform mesh for Example 3.5.3. Tables 3.11-3.13, display the numerical results for a fixed value of $M = 500$ and different choices of pairs (β, α) using nonuniform temporal meshes to achieve the desired accuracy. We

can see from Tables 3.11-3.13 that the proposed scheme (3.45) is computationally efficient and results are in agreement with OC $\min(2-\beta, 3-\alpha, \gamma\beta, \gamma(\alpha-1))$.

TABLE 3.11: Maximum absolute errors and OC in time direction for Example 3.5.3 with different values of β, α, γ and $M = 500$.

	$\gamma = 1$		$\gamma = 2.67$		$\gamma = 4$		
	$\beta = 0.3, \alpha = 1.3$		$\beta = 0.3, \alpha = 1.3$		$\beta = 0.3, \alpha = 1.3$		
τ	$\|u^\tau - U^\tau\|_\infty$	OC	$\|u^\tau - U^\tau\|_\infty$	OC	$\|u^\tau - U^\tau\|_\infty$	OC	CPU(s)
$1/2^5$	1.6647E-02		1.0450E-02		1.9366E-02		1.284360
$1/2^6$	1.3825E-02	0.26794	3.4704E-03	1.5903	4.8003E-03	2.0124	1.886483
$1/2^7$	1.1705E-02	0.24015	1.7827E-03	0.96107	1.2554E-03	1.9349	2.934278
$1/2^8$	9.8867E-03	0.24362	1.0683E-03	0.73871	3.4401E-04	1.8677	4.971753
$1/2^9$	8.2777E-03	0.25625	6.2599E-04	0.77113	9.9921E-05	1.7836	11.14403
$1/2^{10}$	6.8687E-03	0.26921	3.6299E-04	0.78620	3.1286E-05	1.6753	31.48197

In Figure 3.6, plot 3.6**(a)** shows the effect of mesh grading parameters γ's on the absolute error for a non-smooth exact solution in Example 3.5.3. We take particular choice of pair $(\beta, \alpha) = (0.5, 1.5)$ and different $\gamma = 1,\ 1.67,\ 2,\ 2.22$ with $M = N = 50$. One can note from Figure 3.6**(a)** that the error decreases for choice of nonuniform mesh in approximation method. In Figure 3.6**(b)**, we compare the exact and approximate solutions on nonuniform meshes taking $\gamma = 4$ for Example 3.5.3 with $\beta = 0.5$, $\alpha = 1.5$, $M = 33$, and $N = 20$ at final time level $T = 1$.

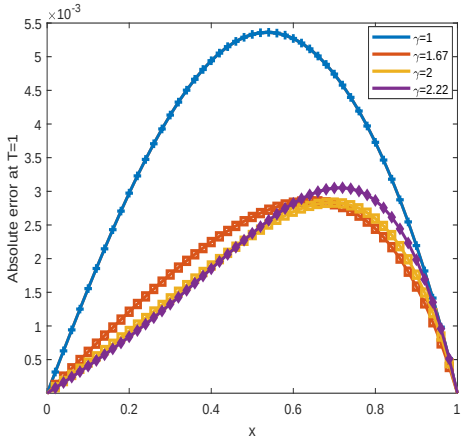

(a) Scheme (3.45) with $\gamma = 1$ and $M = N = 50$.

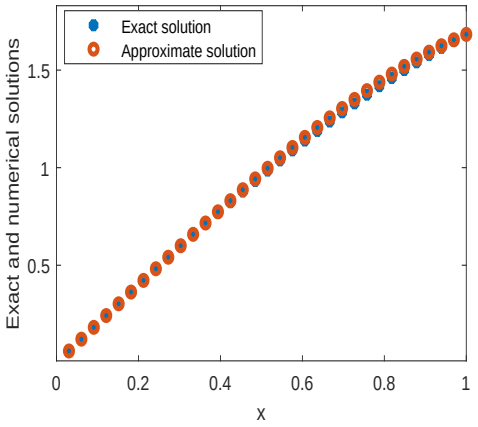

(b) Scheme (3.45) with $\gamma = 4$, $M = 33$, $N = 20$.

FIGURE 3.6: Graph of absolute error (left panel) and, exact and numerical solutions (right panel) at final time $T = 1$ for Example 3.5.3 with $\beta = 0.5$, $\alpha = 1.5$.

TABLE 3.12: Maximum absolute errors and OC in time direction for Example 3.5.3 with different values of β, α, γ and $M = 500$.

	$\gamma = 1$		$\gamma = 2.5$		$\gamma = 1.67$		
	$\beta = 0.5, \alpha = 1.5$		$\beta = 0.5, \alpha = 1.5$		$\beta = 0.8, \alpha = 1.8$		
τ	$\|u^\tau - U^\tau\|_\infty$	OC	$\|u^\tau - U^\tau\|_\infty$	OC	$\|u^\tau - U^\tau\|_\infty$	OC	CPU(s)
$1/2^5$	1.0940E-02		8.5965E-03		4.5669E-03		1.224926
$1/2^6$	5.4993E-03	0.99229	2.1721E-03	1.9847	1.8530E-03	1.3013	1.747783
$1/2^7$	4.1482E-03	0.40675	5.7657E-04	1.9135	8.0375E-04	1.2050	2.744124
$1/2^8$	3.2101E-03	0.36989	1.6085E-04	1.8418	3.5122E-04	1.1944	4.810063
$1/2^9$	2.4802E-03	0.37217	4.7721E-05	1.7530	1.5431E-04	1.1865	9.626798
$1/2^{10}$	1.8888E-03	0.39296	1.5257E-05	1.6451	6.8047E-05	1.1812	31.41446

In Figures 3.7, we compare surfaces of absolute error between uniform mesh ($\gamma = 1$) and nonuniform mesh ($\gamma = 2.5$) when $\beta = 0.5$, $\alpha = 1.5$, $M = N = 50$ for Example 3.5.3. We can see from Figures 3.7**(a)** and 3.7**(a)** that both the surfaces have different behavior near the singular point $t = 0$. In Figure 3.7**(a)**, we can observe the blows-up behavior of error near the singular point $t = 0$. To handle the weak singularity

near initial time, we use general mesh by choosing $\gamma > 1$ in time discretization process. Figure 3.7**(b)** display the similar error for nonuniform mesh $\gamma = 2.5$, and one can notice that our time discretization method works well with graded mesh.

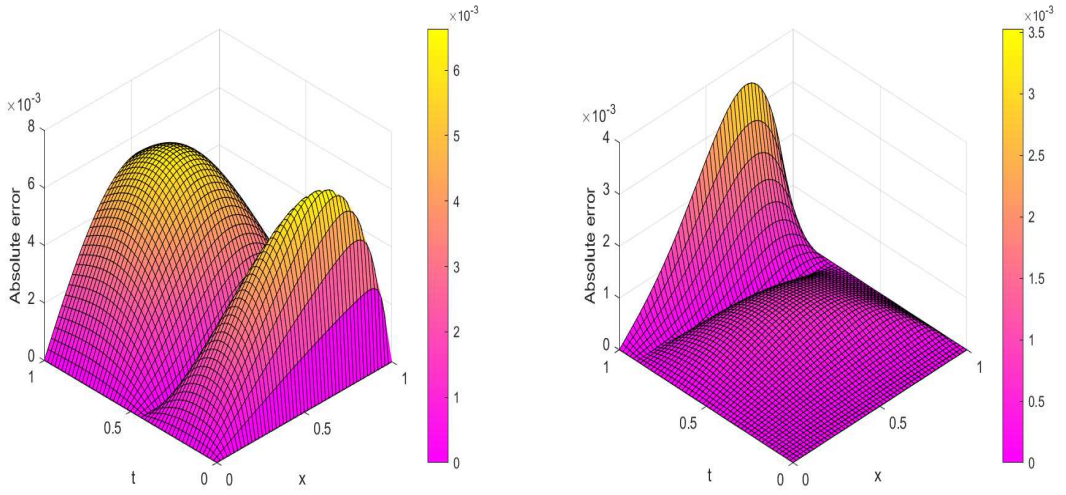

(a) Scheme (3.45) with $\gamma = 1$. **(b)** Scheme (3.45) with $\gamma = 2.5$.

FIGURE 3.7: Absolute error graphs for Example 3.5.3 on the uniform **(a)** and nonuniform **(b)** meshes with $(\beta, \alpha) = (0.5, 1.5)$ and $M = N = 50$.

TABLE 3.13: Maximum absolute errors and OC in time direction for Example 3.5.3 with different values of β, α, γ and $M = 500$.

	$\gamma = 3.5$		$\gamma = 2.14$		$\gamma = 2.14$		
	$\beta = 0.7, \alpha = 1.3$		$\beta = 0.5, \alpha = 1.6$		$\beta = 0.6, \alpha = 1.7$		
τ	$\|u^\tau - U^\tau\|_\infty$	OC	$\|u^\tau - U^\tau\|_\infty$	OC	$\|u^\tau - U^\tau\|_\infty$	OC	CPU(s)
$1/2^5$	1.9015E-02		6.4165E-03		6.1205E-03		1.24999
$1/2^6$	4.9207E-03	1.9502	1.6581E-03	1.9522	2.0175E-03	1.6011	1.79594
$1/2^7$	1.3935E-03	1.8201	4.5500E-04	1.8656	8.0501E-04	1.3255	2.90179
$1/2^8$	4.3119E-04	1.6924	1.3426E-04	1.7608	3.2400E-04	1.3130	5.18547
$1/2^9$	1.4699E-04	1.5526	4.3573E-05	1.6236	1.3122E-04	1.3040	9.88331
$1/2^{10}$	5.5028E-05	1.4175	1.5815E-05	1.4621	5.3354E-05	1.2983	31.0253

Example 3.5.4. We consider 2D Klein-Gordon TFMDW equation on the computational domain $\Omega \times [0,T] = ([0,1] \times [0,1]) \times [0,1]$

$$\begin{cases} {}^{C}\mathcal{D}^{\beta}_{0,t}u(x,y,t) + {}^{C}\mathcal{D}^{\alpha}_{0,t}u(x,y,t) + F(u(x,y,t)) = \frac{\partial^2 u(x,y,t)}{\partial x^2} + \frac{\partial^2 u(x,y,t)}{\partial y^2} + f(x,y,t), \\ u(x,y,t) = 0, \quad \frac{\partial u(x,y,0)}{\partial t} = 0, \quad x,y \in \Omega, \\ u(x,y,t) = (t^{\beta+1} + t^{\alpha})(\sin(1))^2, \quad x,y \in \partial\Omega, \quad t \in (0,T]. \end{cases}$$

The exact solution of considered problem is $u(x,y,t) = (t^{\beta+1} + t^{\alpha})\sin(x)\sin(y)$, $x,y \in \Omega$, $t \in (0,1]$. Then the related source term is defined as:

$$f(x,y,t) = \Big[\Gamma(\beta+2)\, t + \frac{\Gamma(\alpha+1)}{\Gamma(\alpha+1-\beta)}\, t^{\alpha-\beta} + \frac{\Gamma(\beta+2)}{\Gamma(\beta+2-\alpha)}\, t^{\beta+1-\alpha} + \Gamma(\alpha+1) + 2\left(t^{\beta+1} + t^{\alpha}\right)\Big]\sin(x)\sin(y) + F(u(x,y,t)).$$

In Table 3.14, we give the maximum absolute error and convergence order for Example 3.5.4 in the time direction for fixed $h_1 = h_2 = 1/20$, varying N, and different choices of pairs $(\beta,\alpha) = (0.3,1.5),\ (0.7,1.6),\ (0.8,1.4)$ for nonuniform mesh by selecting $\gamma > 1$. In this Table 3.14, we deal with **Case 1** on the domain $[0,1] \times [0,1]$. We can see from Table 3.14 that the temporal accuracy of the current scheme (3.51)-(3.52) agrees with $\min(2-\beta, 3-\alpha, \gamma\beta, \gamma(\alpha-1))$.

TABLE 3.14: Maximum absolute errors and OC in time direction for Example 3.5.4 with different values of β, α, γ and $h_1 = h_2 = \frac{1}{20}$.

	$\gamma = 3.33$		$\gamma = 2$		$\gamma = 3.67$		
	$\beta = 0.3, \alpha = 1.5$		$\beta = 0.7, \alpha = 1.6$		$\beta = 0.8, \alpha = 1.4$		
τ	$\|u^\tau - U^\tau\|_\infty$	OC	$\|u^\tau - U^\tau\|_\infty$	OC	$\|u^\tau - U^\tau\|_\infty$	OC	CPU(s)
$1/2^8$	6.8501E-04		5.1280E-04		1.1696E-03		11.43926
$1/2^9$	3.3671E-04	1.0246	2.5339E-04	1.0171	3.9252E-04	1.5752	56.13212
$1/2^{10}$	1.6259E-04	1.0502	1.2191E-04	1.0555	1.9282E-04	1.0255	348.3140
$1/2^{11}$	7.5626E-05	1.1043	5.5548E-05	1.1340	9.1934E-05	1.0686	1559.488
$1/2^{12}$	3.4541E-05	1.1306	2.2439E-05	1.3078	4.1031E-05	1.1639	7498.723

Figure 3.8 displays the absolute error for Example 3.5.4 using the finite difference scheme defined in (3.51)-(3.52) for different pair of fractional parameters $(\beta, \alpha) = (0.3, 1.5)$ at $T = 1$. Figure 3.8**(a)** expresses the error plot corresponding to uniform discretization $\gamma = 1$ in approximation method (3.51)-(3.52). However, Figures 3.8**(b)**, 3.8**(c)**, 3.8**(d)** show the error plot for nonuniform cases $\gamma = 2$, $\gamma = 3$, $\gamma = 4$, respectively. From these figures we can note the effectiveness of the nonuniform meshes. Figures 3.8**(b)**, 3.8**(c)**, 3.8**(d)** have smooth behavior of absolute error in comparison to Figure 3.8**(a)**. We see that the error is increasing for uniform mesh due to non-smooth nature of boundary condition. In resolving such type of singularities in boundary conditions as well as in solutions, we employ the nonuniform mesh to recover an optimal OC.

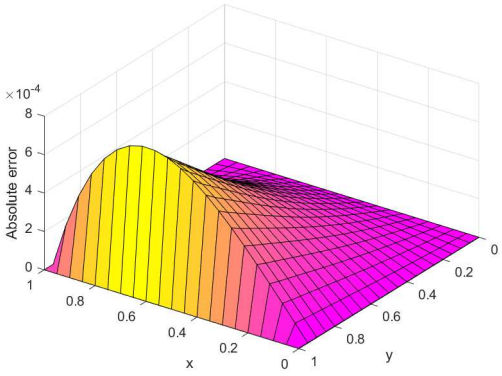

(a) For scheme (3.51)-(3.52) with $\gamma = 1$.

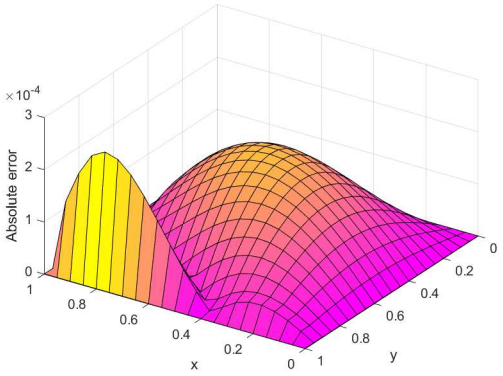

(b) For scheme (3.51)-(3.52) with $\gamma = 2$.

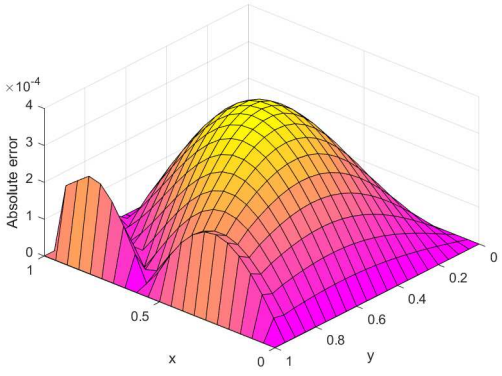

(c) For scheme (3.51)-(3.52) with $\gamma = 3$.

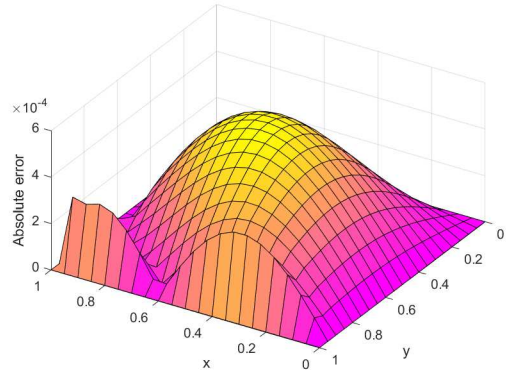

(d) For scheme (3.51)-(3.52) with $\gamma = 4$.

FIGURE 3.8: Graphs of absolute error using ADI scheme (3.51)-(3.52) with $h_1 = h_2 = 1/20$, $\tau = 1/400$, $\beta = 0.3$, $\alpha = 1.5$, $T = 1$ on $\Omega = [0, 1] \times [0, 1]$ with different values of γ for Example 3.5.4.

Table 3.15, present the maximum absolute errors and OC in space direction with $N = 30,000$ and varying M_1, M_2 for Example 3.5.4. Numerical results are discussed for different values of β and α on nonuniform time grids by taking mesh grading parameter $\gamma = 2.67$. We analyze that the numerical results are in agreement with theoretical convergence rate. Table 3.15 shows that the ADI scheme (3.51)-(3.52) is second-order accurate in space direction.

TABLE 3.15: Maximum absolute errors and OC in space direction for Example 3.5.4 with different values of β, α, $\gamma = 2.67$ and $\tau = \frac{1}{30000}$.

	$\beta = 0.5, \alpha = 1.8$		$\beta = 0.5, \alpha = 1.5$		$\beta = 0.4, \alpha = 1.6$	
M	$\|u^\tau - U^\tau\|_\infty$	OC	$\|u^\tau - U^\tau\|_\infty$	OC	$\|u^\tau - U^\tau\|_\infty$	OC
4	3.8119E-04		3.7501E-04		3.8169E-04	
8	1.0461E-04	1.8655	1.0453E-04	1.8431	1.0584E-04	1.8505
16	2.4791E-05	2.0771	2.7165E-05	1.9440	2.7060E-05	1.9676

Example 3.5.5. Consider the nonlinear Klein and Sine-Gordon TFMDW equation in 1D and 2D with the following exact solution

$$u(X_r, t) = t^\rho \exp\left(-\frac{(X_r - \zeta)^2}{\Psi}\right), \ r = 1, 2, \ X_1 \equiv x, \ X_2 \equiv (x, y), \ X_r \times t \in \Omega \times [0, 1].$$

Then the initial and boundary conditions are

$$u(X_r, 0) = 0 = u_t(X_r, 0), \quad r = 1, 2, \ X_r \in \Omega,$$

$$u(X_r, t) = t^\rho \exp\left(-\frac{(X_r - \zeta)^2}{\Psi}\right), \quad (X_r, t) \in \partial\Omega \times (0, 1].$$

and the source term is

$$\begin{aligned} f(X_r, t) = &\left(\frac{\Gamma(\rho+1)}{\Gamma(\rho+1-\beta)} t^{\rho-\beta} + \frac{\Gamma(\rho+1)}{\Gamma(\rho+1-\alpha)} t^{\rho-\alpha} + \frac{2}{\Psi} t^\rho \right. \\ &\left. - \frac{4}{\Psi^2}(X_r - \zeta)^2 t^\rho\right) \exp\left(-\frac{(X_r - \zeta)^2}{\Psi}\right) + F(u(X_r, t)). \end{aligned}$$

Tables 3.16 and 3.17 describe the absolute error and OC of one and 2D cases for Example 3.5.5, respectively. Table 3.16 represents the error on L_∞ norm and OC for both temporal and space directions by using the scheme (3.45). In this Table, we fix $M = 2000$, varying N, and fix $N = 2000$, varying M to get the numerical results

in temporal and space directions, respectively. In Table 3.16, we use nonlinear term $F(u) = u^2$, $\zeta = 0.5$, $\Psi = 0.02$ with different values of β, α, and γ to handle the nonsmooth nature of the exact solution on the domain $\Omega \times [0, T] = [0, 1] \times [0, 1]$. In Table 3.17, we display the absolute error on the L_∞ norm and OC on the temporal side by using the scheme (3.51)-(3.52). Table 3.17 shows the numerical results for $F(u) = \sin(u)$, $\zeta = 50$, $\Psi = 100$ with different pairs (β, α) on the domain $\Omega \times [0, T] = [0, 100] \times [0, 100] \times [0, 1]$. Tables 3.16 and 3.17 confirm that the numerical schemes (3.45) and (3.51)-(3.52) provide good accuracy for both directions.

TABLE 3.16: Maximum absolute errors and OC in time ($M = 2000$) and space ($N = 2000$) directions for Example 3.5.5 (1D case) with different values of β, α, γ, $\rho = \alpha$, $\zeta = 0.5$ and $\Psi = 0.02$, $F(u) = u^2$.

	$\gamma = 14/5$		$\gamma = 3/2$		$\gamma = 13/7$		$\beta = 0.4$
	$\beta = 0.5, \alpha = 1.6$		$\beta = 0.4, \alpha = 1.8$		$\beta = 0.3, \alpha = 1.7$		$\alpha = 1.8$
τ	$\|u^\tau - U^\tau\|_\infty$	OC	$\|u^\tau - U^\tau\|_\infty$	OC	$\|u^\tau - U^\tau\|_\infty$	OC	CPU(s)
$1/2^6$	4.0778E-04		8.7445E-04		6.0008E-04		9.025324
$1/2^7$	1.6071E-04	1.3434	3.8323E-04	1.1902	2.3855E-04	1.3309	31.23791
$1/2^8$	6.2901E-05	1.3533	1.6733E-04	1.1956	9.5195E-05	1.3253	77.08585
$1/2^9$	2.4340E-05	1.3697	7.2838E-05	1.1999	3.8018E-05	1.3242	166.6383
$1/2^{10}$	9.2273E-06	1.3994	3.1582E-05	1.2056	1.5102E-05	1.3320	314.9025
$1/2^{11}$	3.5192E-06	1.3907	1.3603E-05	1.2152	6.0159E-06	1.3279	767.3831
	$\gamma = 3$		$\gamma = 14/5$		$\gamma = 13/6$		$\beta = 0.7$
	$\beta = 0.8, \alpha = 1.4$		$\beta = 0.6, \alpha = 1.5$		$\beta = 0.7, \alpha = 1.6$		$\alpha = 0.6$
h	$\|u^\tau - U^\tau\|_\infty$	OC	$\|u^\tau - U^\tau\|_\infty$	OC	$\|u^\tau - U^\tau\|_\infty$	OC	CPU(s)
$1/2^4$	3.2919E-02		3.2923E-02		3.2898E-02		6.090590
$1/2^5$	7.8612E-03	2.0661	7.8574E-03	2.0669	7.8524E-03	2.0668	11.53135
$1/2^6$	1.9493E-03	2.0118	1.9438E-03	2.0151	1.9436E-03	2.0144	17.66998
$1/2^7$	4.9172E-04	1.9871	4.8579E-04	2.0005	4.8669E-04	1.9976	26.07127

Figure 3.9 demonstrates the absolute error for a nonsmooth solution of Example 3.5.5 using the method defined in (3.45). In this Figure, we plot the surface of error for $(\beta, \alpha) = (0.5, 1.5)$ and $M = N = 50$ with different values of grading parameter γ. The effect of the nonuniform meshes near the singularity at $t = 0$ can be observed from these Figures 3.9**(a)** and 3.9**(b)**. In Figure 3.9**(a)**, the error behavior blows up near the singularity $t = 0$. However, this behavior of error is tackled in Figure 3.9**(b)** by selecting a suitable choice of parameter γ.

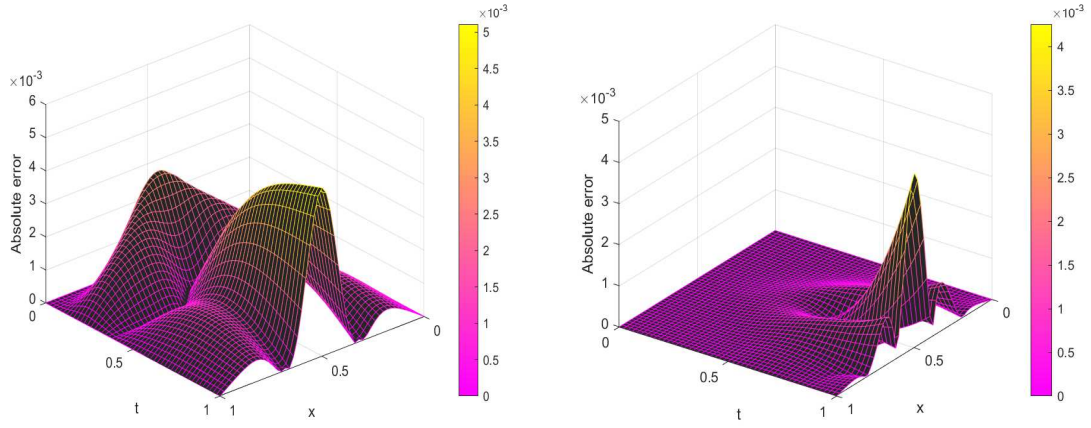

(a) Scheme (3.45) with $\gamma = 1$.

(b) Scheme (3.45) with $\gamma = 3$.

FIGURE 3.9: Absolute error graphs for Example 3.5.5 on the uniform **(a)** and nonuniform **(b)** meshes with $(\beta, \alpha) = (0.5, 1.5)$ $(\zeta, \Psi) = (0.5, 0.02)$ and $M = N = 50$.

TABLE 3.17: Maximum absolute errors and OC in time direction for Example 3.5.5 (2D case) with different values of β, α, $\rho = 3$, $\zeta = 50$ and $\Psi = 100$, $F(u) = \sin(u)$.

	$\beta = 0.5, \alpha = 1.5$		$\beta = 0.5, \alpha = 1.7$		$\beta = 0.85, \alpha = 1.3$		
τ	$\|u^\tau - U^\tau\|_\infty$	OC	$\|u^\tau - U^\tau\|_\infty$	OC	$\|u^\tau - U^\tau\|_\infty$	OC	CPU(s)
$1/2^2$	1.2333E-01		1.7721E-01		1.5049E-01		0.527258
$1/2^3$	4.2854E-02	1.5250	6.9380E-02	1.3528	5.9737E-02	1.3330	1.594473
$1/2^4$	1.4914E-02	1.5228	2.7353E-02	1.3428	2.4714E-02	1.2733	4.128901
$1/2^5$	5.2105E-03	1.5172	1.0835E-02	1.3360	1.0520E-02	1.2322	10.67341
$1/2^6$	1.8348E-03	1.5058	4.3138E-03	1.3287	4.5699E-03	1.2029	30.42070

Example 3.5.6. In this example, we consider 2D Klein-Gordon TFMDW equation on the domain $(x, y, t) \in \Omega \times [0, 1]$

$$\begin{cases} {}^C\mathcal{D}^{\beta}_{0,t}u(x,y,t) + {}^C\mathcal{D}^{\alpha}_{0,t}u(x,y,t) + u^3(x,y,t) - 2u(x,y,t) = \Delta u(x,y,t) + f(x,y,t), \\ u(x,y,0) = 0, \quad \frac{\partial u(x,y,0)}{\partial t} = 0, \quad x, y \in \Omega, \\ u(x,y,t) = t^5 \cos(\pi x)\cos(\pi y), \quad x, y \in \partial\Omega, \quad t \in (0, T], \end{cases}$$

with source term

$$f(x,y,t) = \left[\frac{5!}{\Gamma(6-\beta)}t^{5-\beta} + \frac{5!}{\Gamma(6-\alpha)}t^{5-\alpha} + 2\pi^2 t^5\right]\cos(\pi x)\cos(\pi y) + (t^5\cos(\pi x)\cos(\pi y))^3 - 2(t^5\cos(\pi x)\cos(\pi y)).$$

It this case, the analytic solution is $u(x, y, t) = t^5 \cos(\pi x)\cos(\pi y)$, x, $y \in \Omega$. We solve this equation (3.1) by using ADI difference scheme (3.51)-(3.52) on the domain $\Omega \times [0, T] = [0, 1] \times [0, 1] \times [0, 1]$. In Table 3.18, we display the numerical results with different values of $\beta = 0.3$, 0.5, 0.8 and $\alpha = 1.8$ for Example 3.5.6. We observe that

the convergence rate agrees with the temporal accuracy which is $\min(2-\beta, 3-\alpha) = 1.20$ for the choice of β and α.

TABLE 3.18: Maximum absolute errors and OC in time direction for Example 3.5.6 with different values of β, $\alpha = 1.8$ and $M_1 = M_2 = N$.

	$\beta = 0.3$		$\beta = 0.5$		$\beta = 0.8$		
τ	$\|u^\tau - U^\tau\|_\infty$	OC	$\|u^\tau - U^\tau\|_\infty$	OC	$\|u^\tau - U^\tau\|_\infty$	OC	CPU(s)
1/5	5.2675E-02		5.2699E-02		5.4911E-02		0.054558
1/10	2.1215E-02	1.3120	2.1369E-02	1.3023	2.2534E-02	1.2850	0.122206
1/20	6.1250E-03	1.7923	6.1936E-03	1.7866	7.3124E-03	1.6237	0.457092
1/40	2.5477E-03	1.2655	2.6427E-03	1.2288	3.2341E-03	1.1770	5.851943

In Tables 3.19 and 3.20, we present the numerical results in space direction for Examples 3.5.3 and 3.5.6, respectively with different choice of pairs (β, α) and fixed time step size $\tau = \frac{1}{15000}$. Table 3.19 shows the maximum absolute error and OC on nonuniform meshes by using $\gamma = 2.67$, whereas in Table 3.20 the numerical results are given with uniform meshes. From Tables 3.19 and 3.20, we can observe that the scheme for 1D case (3.45) as well as for 2D case (3.51)-(3.52) is second order accurate in space.

TABLE 3.19: Maximum absolute errors and OC in space direction for Example 3.5.3 with $F(u) = u^3 - 2u$, varying values of β, α, $\gamma = 2.67$ and $\tau = \frac{1}{15000}$.

	$\beta = 0.3, \alpha = 1.6$		$\beta = 0.5, \alpha = 1.5$		$\beta = 0.4, \alpha = 1.6$		
$M_1 = M_2$	$\|u^\tau - U^\tau\|_\infty$	OC	$\|u^\tau - U^\tau\|_\infty$	OC	$\|u^\tau - U^\tau\|_\infty$	OC	CPU
3	8.1391E-04		7.7763E-04		7.4013E-04		2159
6	2.1783E-04	1.9017	2.0498E-04	1.9236	1.9594E-04	1.9174	4339
12	5.7831E-05	1.9133	5.2308E-05	1.9704	5.2038E-05	1.9128	6535

TABLE 3.20: Maximum absolute errors and OC in space direction for Example 3.5.6 with $F(u) = u^3 - 2u$, varying values of β, α, $\gamma = 1$ and $\tau = \frac{1}{15000}$.

	$\beta = 0.3, \alpha = 1.8$		$\beta = 0.5, \alpha = 1.5$		$\beta = 0.4, \alpha = 1.6$	
$M_1 = M_2$	$\|u^\tau - U^\tau\|_\infty$	OC	$\|u^\tau - U^\tau\|_\infty$	OC	$\|u^\tau - U^\tau\|_\infty$	OC
4	6.0666E-03		6.5495E-03		6.4245E-03	
8	1.7071E-03	1.8293	1.8062E-03	1.8584	1.7803E-03	1.8515
16	4.7527E-04	1.8448	5.0116E-04	1.8496	4.9411E-04	1.8492
32	1.2233E-04	1.9579	1.2732E-04	1.9768	1.2567E-04	1.9752

3.6 Conclusion

We discussed an efficient difference schemes based on ADI approach for solving the 2D nonlinear TFMDW equation. We proposed nonuniform $L1$ approximation method by using discretization process based on half grid subintervals of domain $[0, T]$ defined in (3.8) to approximate the TFCDs of order β $(0 < \beta < 1)$ and α $(1 < \alpha < 2)$ in equation (3.1). This approximation method has an advantage in numerical accuracy over the methods on uniform discretization. The nonuniform $L1$ method is used for the approximation of the time-fractional derivatives, and central difference approximation for the space derivative to get an equivalent system of equations of the considered model (3.1)-(3.3). The local truncation error bound is shown for time-fractional derivative approximation methods. The theoretical investigation describes that the derived scheme has convergence rate $\min(2-\beta,\ 3-\alpha,\ \gamma\beta,\ \gamma(\alpha-1))$ in time and second order in space direction, and it is unconditionally stable for $\beta \in (0, 1)$ and $\alpha \in (1, 2)$. Numerical examples show that the difference scheme confirms the OC in time and space direction, and works well for finding the numerical solutions to high-dimensional problems. The current numerical algorithm handles the weak

singularity at $t = 0$ i.e. when exact solution is non-smooth for the governing problem (3.1)-(3.3). We presented several numerical examples with zero as well as non-zero boundary conditions corresponding to smooth and non-smooth exact solutions of the considered problem.

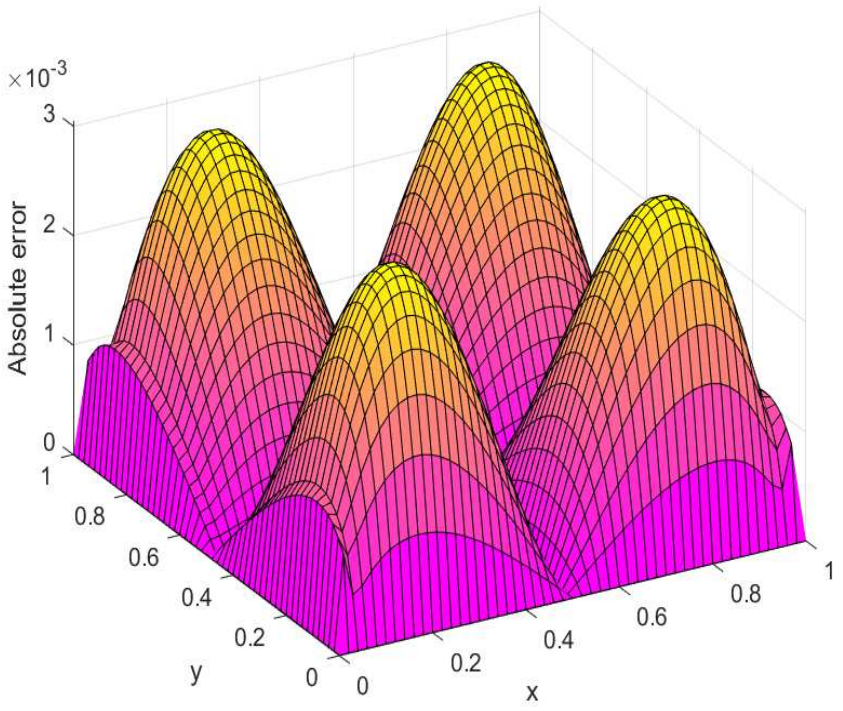

FIGURE 3.10: Absolute error graphs for Example 3.5.6 using the scheme (3.51)-(3.52) with $M_1 = M_2 = N = 80$ and $\beta = 0.85$, $\alpha = 1.85$.

****